Recent trends in design, manufacturing and challenges of bone-like bioceramic scaffolds

Ceramics International 51 (2025) 12355–12369

Contents lists available at ScienceDirect

Ceramics International

journal homepage: www.elsevier.com/locate/ceramint

Recent trends in design, manufacturing and challenges of bone-like bioceramic scaffolds

Francesco Baino [a,*], Roberta Gabrieli [a], Enrica Verné [a], Alessandro Schiavi [b], Martin Schwentenwein [c], Luca D'Andrea [d], Pasquale Vena [d]

[a] Institute of Materials Physics and Engineering, Department of Applied Science and Technology, Politecnico di Torino, Turin, Italy
[b] National Institute of Metrological Research (INRiM), Applied Metrology and Engineering Division, Turin, Italy
[c] Lithoz GmbH, Vienna, Austria
[d] Department of Chemistry, Materials and Chemical Engineering "Giulio Natta", Laboratory of Biological Structure Mechanics (LaBS), Politecnico di Milano, Milan, Italy

ARTICLE INFO

Handling Editor: Dr P. Vincenzini

Keywords:
Biomedical applications
Bioceramics
Porosity
Additive manufacturing

ABSTRACT

Biomaterials are often produced in the form of porous scaffolds acting as templates to allow tissue growth and regeneration in 3D. Structural biomimicry is a commonly-followed criterion so that the scaffold can replicate the trabecular architecture of bone. This is a particularly difficult task when bioactive ceramics and glasses are used for osseous applications due to some challenges related to the inherent characteristics of the materials and relevant fabrication processes (e.g. reproducibility, reliability and the need for consolidation via high-temperature sintering). Recent progresses in the advanced manufacturing of bioactive ceramics and glasses have allowed researchers to overcome some of these limitations. Given such a scenario, this review paper – which is organized in four major sections – aims to critically discuss the strategies to optimize bioceramic scaffold design and evaluate its suitability for bone applications. After an introduction to the context, section 2 provides an overview of the requirements that a porous bioceramic scaffold should ideally fulfil. Different options for scaffold fabrication, ranging from conventional methods to additive manufacturing technologies, are critically discussed in section 3. Section 4 is addressed to the strategies developed to integrate the design of bone-like structures, also driven by computational tools, into additive manufacturing methodologies. Section 5 focuses on how quantifying the "bone similarity" of scaffolds or, more generally, how assessing if a scaffold is truly suitable for bone applications; advantages and limitations of the current approaches are discussed along with an outlook for future challenges.

1. Introduction

Critical size bone defects (i.e., larger than 2 cm in length and with more than 50 % circumferential bone loss [1]) refer to a serious clinical condition affecting the elderly as well as young population. Current clinical approaches to treat such defects involve the transplantation of autografts or allografts, or the implantation of synthetic bone substitutes. All these existing solutions suffer from some limitations: autografts are constrained by donor site morbidity and limited availability, allografts carry the risk of immune rejection and disease transmission as well as may arise ethical or religious concerns especially for some cultures, while synthetic materials may lack adequate bioactivity or not possess the mechanical strength necessary to support load-bearing applications [2]. Overall, these conditions may cause low quality of life and long hospitalization periods with high costs on healthcare systems, thereby creating a major societal and economic problem [3]. The development of bioceramic and, especially, bioactive scaffolds is one of the cornerstones to approach these clinical challenges [4]. Bioceramic scaffolds can be effectively used to treat critical size bone defects in cases of trauma or tissue removal upon surgery. For such large defects, bone cannot heal spontaneously and a mechanical supporting device able to promote the formation of new bone needs to be implanted. Both trabecular and cortical bone can be involved in the treatment, bringing to different and specific requirements in the design of the bone substitute material.

Bone tissue exhibits a complex, multilevel organization with

This article is part of a special issue entitled: CIMTEC 2024 published in Ceramics International.

* Corresponding author.
E-mail address: francesco.baino@polito.it (F. Baino).

https://doi.org/10.1016/j.ceramint.2025.02.307
Received 15 September 2024; Received in revised form 19 February 2025; Accepted 21 February 2025
Available online 21 February 2025

multiscale porosity [5] that is difficult to replicate using man-made biomaterials. Bone substitutes are often produced as 3D porous templates (scaffolds) that guide new tissue formation and are eventually resorbed or integrated into the body. An ideal scaffold must mimic the natural bone environment, providing mechanical support, biocompatibility, and promoting cellular activities. Various materials, including bioactive ceramics and glasses, polymers, metals and composites, are used to fabricate scaffolds that imitate the structure and function of bone tissue [6]. As bone substitutes, bioactive materials have the ability to chemically bond to the bone and form a tight interface that can stimulate new bone formation [7]. These materials are biointegrated with or even replaced by healthy tissue, promoting the adhesion and proliferation of bone cells [8,9]. Bioceramics exhibit similar rigidity and physico-mechanical properties to those of bone. Hydroxyapatite and other calcium phosphates have crystallographic and/or compositional similarity to the mineral component of bone [10], while bioactive glasses are prone to be coated with a nanocrystalline apatite-like phase once implanted in vivo, thus developing a "biomimetic skin" that is favourable for osteoblast adhesion and proliferation [11,12], and can also release ions with osteostimulatory properties [13]. In addition to calcium phosphates and bioactive glasses, which are commercially available and FDA-approved since decades [14], other bioceramics, such as silicon nitride and baghdadite, have recently emerged as potential candidates for scaffold fabrication. However, there are some barriers to their clinical application due to factors such as synthesis/fabrication challenges and insufficient research on their long-term biocompatibility and mechanical performance [15–17]. Besides the biomaterial composition, the pore architecture of the scaffold – which depends on the fabrication method – also plays a pivotal role in dictating the implant performances. Hence, this work aims to shed light on the design–fabrication–pore structure–biomechanical performance relationships in bioceramic scaffolds, as well as on the methods to reliably estimate the "bone-biomimicry" and actual suitability of these porous implants.

2. Ideal requirements for bone tissue engineering scaffolds

Over the last decades, the need for synthetic bone grafts impressively increased as a less-invasive, more abundant and safer alternative to osseous transplantation from humans (autografts and allografts) or animals (xenografts) [18]. In this regard, implantable biomaterials for bone repair and regeneration are often produced in the form of porous templates (scaffolds) that simply support (osteoconduction) or even stimulate (osteoinduction) the growth of healthy bone in 3D (osteogenesis), provided that in the latter case they are inherently bioactive [19].

Despite the latest advances in both material development and manufacturing technologies, the fabrication of a truly ideal scaffold for bone tissue engineering is still challenging considering the multiple requirements that it should exhibit, as summarized in Table 1.

Biocompatibility and bioactivity requirements are the easiest ones to be satisfied being mainly related to the inherent properties of scaffold biomaterials rather than the porous structure. Many different biomaterials are now available for bone tissue engineering applications and, therefore, both properties can be accomplished once the basic material for scaffolding has been selected [20]. From a general viewpoint, metals, ceramics, glasses, natural or synthetic polymers, and composites all potentially suitable for making scaffolds; however, metallic and polymeric biomaterials are typically inert or almost inert and, thus, unable to actively stimulate bone regeneration as bioactive ceramics and glasses can do [21]. Specific details about the inherent bone-regenerative capability and properties of biomedical glasses, crystalline ceramics and bio-composites can be found elsewhere [22–24]. An emerging aspect that is attracting great interest concerns biomaterial- or scaffold-related immunomodulation, as immune cells and their factors play a pivotal role in the foreign body reaction following implant placement, the clearance of dead cells and the regeneration and overall healing of bone tissue [25].

Table 1
List of the minimum requirements that a bone scaffold should match in order to be used in bone tissue engineering.

Requirement	Short description
Biocompatibility	- Promotion of cell adhesion and proliferation - Promotion of cell differentiation and migration - Promotion of ECM synthesis - Proper modulation of immune response - No release of toxic degradation products
Bioactivity	- Creation of a stable interface with the host tissue - Promotion of bone cell activity and osteogenesis
Biodegradability	- Comparable with the physiological healing time of the tissue
Mechanical properties	- Comparable with those of host bone - Mechanical integrity ensured during degradation and tissue remodeling
3D structure	- Open-cell architecture and high interconnectivity - Promotion of mass transport - Support of cell migration, vascularization and bone ingrowth
Manufacturability and related aspects	- Cost effectiveness of the technology used - Scalability - Repeatability/reliability - Sterilization, safe delivery and storage of the final product - Low environmental impact

A further key aspect related to scaffolds – partially associated to bioactivity – is related to material degradability in contact with body fluids [26]. In fact, in a typical tissue engineering approach, the scaffold has not to be intended as a permanent implant – like metallic joint prostheses – but it should gradually dissolve in order to be replaced by new regenerated tissue. Scaffold degradation rate should match the healing rate of bone that depends on multiple variables, including patient's characteristics (age, sex and general health conditions) and anatomical factors (site of concern, specific type of bone considered, etc.). For example, it is known that, in young individuals, bone fractures normally heal to the point of weight-bearing in about 6 weeks with complete recovery of the mechanical integrity achieved approximately 1 year after fracture, but in the elderly the rate of repair slows down [27]. This indicates that the material selection should also take into account clinical parameters and age of the subjects.

Another critical aspect to be considered when designing scaffolds for bone regeneration is the achievement of a right balance between mechanical properties (especially stiffness and strength) and adequate porosity, which are both key features to induce the physiological growth of new bone. In fact, as the total porosity and mean pore size of the scaffolds increase, the elastic modulus and mechanical strength decrease; on the other hand, however, large and interconnected pores in the range of some hundreds of micrometres favour tissue ingrowth and vascularization of the bone substitute [28]. Typical ranges of mechanical properties recommended for bone scaffolds are those of trabecular bone, e.g. 0.1–16 MPa for the compressive strength [29] and 50–500 MPa for the elastic modulus [30]. Furthermore, one of the most critical aspects from a mechanical viewpoint – especially in load-bearing applications – is the achievement of a suitable primary stability of the implant as soon as possible after surgery [31]. Hence, having a good matching between the mechanical properties of the scaffold and the surrounding tissue is key to satisfy the physiological demand of native bone without inducing tissue resorption; in fact, bone cells act as mechano-transducers, modulating their metabolism as a consequence of the stimuli received. It has been reported that the stimuli derived from scaffold deformation are able to highly influence osteoinductive phenomena and this is the reason why the modulation of fluid flow within the scaffolds has been proposed for triggering mechano-transduction strategies [32].

With regard to pore characteristics, 3D scaffolds should exhibit a

highly interconnected porous structure suitably designed to allow cell penetration and guarantee bone-like mass transport properties. An open-cell architecture is key to permit the supply of oxygen and nutrients as well as the elimination of waste by-products from the core of the scaffold [33]. Pore sizes have to be carefully designed in order to be large enough for promoting cell migration into the scaffold and small enough for having a sufficiently high surface area to reach a critical cellular density on the scaffold. The minimum pore size and total porosity of implantable scaffolds required to regenerate bone are generally recommended to be around 100 μm and 50 vol%, respectively. These two values were first proposed as the best ones in the seminal study of Hulbert et al. [34] in 1970, where calcium aluminate cylindrical implants with 46 vol% porosity and different pore sizes were implanted in dog femora. It was observed that large pores within 100–150 and 150–200 μm yielded significant bone ingrowth, while pores in the range of 75–100 μm resulted in the ingrowth of unmineralized osteoid tissue, and smaller pores (44–75 and 10–44 μm) were infiltrated only by fibrous tissue. Although the two values reported above are still considered as reference thresholds for bone scaffolds, there is a couple of special cases deserving to be mentioned. In fact, those values were originally proposed for almost-inert ceramic scaffolds ("passive" bone in-growth) but, if inherently osteoinductive materials such as bioactive glasses are used, the role played by pore size may not be so important as the ionic dissolution products released over time can exert an osteogenic effect in vivo regardless of the pore size [13]. Furthermore, if the material is resorbable, the pore size and total porosity can increase over time, also changing the characteristics of the 3D structure and, hence, the biological properties of the scaffold [35].

From a general viewpoint, large pores with diameter from 100 to 500 μm are recognized to be useful to promote cell migration, proliferation and differentiation through the entire 3D volume of the scaffold, neovascularization and to improve mass transport of oxygen and nutrient [36–38]. With regard to specific studies about β-TCP scaffolds, it was shown that the growth of blood vessels is limited in pores with size below 400 μm [39] and giant pores larger than 1200 μm discourage osteoconduction [40]. It was also shown that pores smaller than 20 μm may cause fibrous tissue formation around the scaffold, which physically prevents angiogenesis [41,42]; thus, the number of pores close to this size should be somehow limited. On the other hand, smaller pores at the micrometric or even nanometric scale on the surface of scaffold struts can create a diffused micro-/nano-roughness fostering osteoblast adhesion [43]. In summary, the presence of a bimodal pore distribution (large interconnected macropores and small micropores on the struts and walls) in the implanted scaffold is overall considered beneficial for the development of new functional bone (see also Fig. 1).

Another key parameter describing the porous structure and dictating the biological performance of scaffolds is the intrinsic permeability. A minimum value of 3×10^{-11} m^2 was reported to be the permeability threshold to ensure scaffold vascularization and proper mineralization of the newly formed tissue [44,45] (Fig. 2); further details on these aspects will be discussed in section 5.

Finally, the scaffolds should be manufacturable by using affordable, reproducible and reliable technologies in order to scale up the production process while limiting the costs and guaranteeing high quality levels of the final products (see section 3). It is fundamental to develop manufacturing processes responding to good manufacturing practice standards to favour the spread of tissue engineering in the clinic. Among the other factors, delivery and storage (e.g. in a water-proof environment) of the final products have to be well defined in order to preserve scaffold integrity and functionality.

3. Fabrication strategies

3.1. Conventional ("non-printing") methods

According to the literature, the first bioceramic scaffold with an intentionally-created internal macroporosity was fabricated in 2001 and actually consisted of 45S5 bioactive glass porous cylinders obtained via H_2O_2 foaming followed by sintering [46]. These early scaffolds were implanted in dogs to promote bone regeneration but suffered from poor interconnectivity of the pores. Since then, many processing routes have been proposed for fabricating more performant bioactive ceramics and glass scaffolds, as comprehensively reviewed elsewhere [47–49]. A concise overview of the methods is also provided in Table 2 and some examples are shown in Fig. 3. Indeed, the same technique may yield scaffolds with different characteristics in terms of porosity, mechanical and biological properties if applied to different materials, and depending on the processing parameters (e.g. sintering temperature) adopted for obtaining a specific product. Among the various technologies, the space holder method is one of the simplest ones and involves mixing glass powders with a solid polymeric phase of natural (e.g. rice husk [50]) or synthetic origin (e.g. polyethylene microbeads [51,52]) which acts as a thermally-removable pore-forming agent; the scaffolds produced by this technique generally exhibit high mechanical strength (even above 100 MPa under compression) due to the presence of thick struts, quite low porosity (25–50 vol%) and poor interconnectivity of pores. Different types of starches can also be used as swellable pore-forming substances in a more complex variant of the method [53], which was originally developed for non-biomedical applications [54].

More porous scaffolds were obtained through the foaming of inorganic sols by using surfactants acting as bubbling agents [75,56]: this method, which is typically applied to sol-gel bioactive glasses, yields highly-porous foams with interconnected spherical pores but the resulting structures have poor mechanical strength due to the inherent

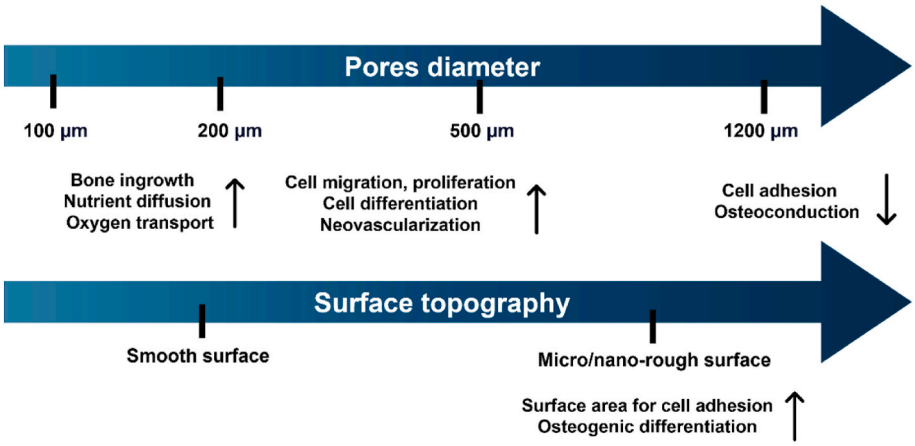

Fig. 1. Functions of the different pore sizes and surface roughness in scaffolds for bone tissue engineering.

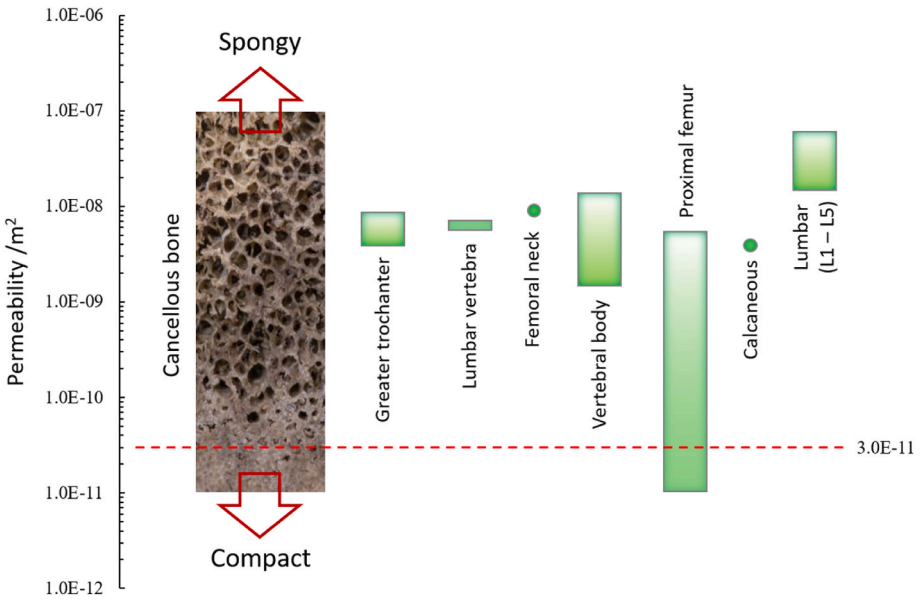

Fig. 2. Comparison of permeability values for different human bone types.

nanoporosity generated by the sol-gel process.

Freezing approaches were also proposed with very interesting results. In this regard, super-tough scaffolds with nacre-like structure were produced by suspending ceramic particles in water and then freezing the system under a controlled thermal gradient [76]. Strong structures with oriented columnar pores mimicking the cortical bone were also obtained by the unidirectional freezing of camphene-based bioactive glass suspensions [63]: these scaffolds were shown to exhibit good bone regenerative ability once implanted in rat calvarial defects [77].

Perhaps the most cost-effective, simple and versatile "conventional" technique to produce truly bone-like bioactive ceramic and glass scaffolds is the sponge replica method, which relies on the impregnation of an open-cell porous template of natural (e.g. marine sponge [78,58]) or synthetic origin synthetic (e.g. polyurethane sponge [60,79]) with a slurry of micrometric or submicrometric ceramic or glass particles along with small amounts of polymeric binding agents. After subsequent sintering, a porous scaffold with the same architecture of the sacrificial template is obtained. Over the years, the process was optimized to improve the mechanical properties and obtain strong foam-like scaffolds with compressive strength up to 20 MPa [61]. A comprehensive discussion of the pros and cons of this method is reported elsewhere [80].

All the "conventional" methods described above for obtaining entirely glass or ceramic porous biomaterials are typically followed by a thermal stage of high-temperature sintering in order to consolidate the final structure of the scaffold while removing all the organic substances. An exception is represented by inorganic-organic biphasic biomaterials: if the "survival" of the polymer is a goal to produce softer polymer/ceramic or polymer/glass porous composites, methods like thermally-induced phase separation or solvent-casting and particulate leaching can be used in which the thermal treatment is skipped [64,65,81] (see Table 2).

3.2. Additive manufacturing

The last frontier in terms of scaffold fabrication relies on the use of 3D printing approaches, which potentially allow achieving a great control on pore geometry and architecture (Table 2). This group of processing methods involves the use of layer-by-layer fabrication approaches to obtain porous structures with customized external shape and pre-designed internal architecture [82]. The starting point in all additive manufacturing technologies is a model from computer-aided design (CAD) or computed tomography (CT) of the object that has to be reproduced. Then, this 3D virtual model is sliced into layers along one of its axes and the 3D printer builds the object making each layer, one by one, according to a layer-wise strategy. In this way, porous products with complex shapes can be obtained to match bone defects with irregular anatomy [82]. With regard to bioactive ceramics and glasses, selective laser sintering, vat photopolymerization (also commonly known as stereolithography) and extrusion-based techniques (e.g. robocasting) have shown a great potential. A comprehensive overview of additive manufacturing techniques applied to ceramic materials can be found elsewhere [83].

3D printing machines for selective laser sintering and vat photopolymerization often have high investment costs, especially if used for mass production, which relatively limit their widespread use in biomedicine. Some extrusion-based 3D printers for industrial-scale applications can also be expensive, but smaller machines are typically cheaper and indeed allow processing a wide range of ceramic- and glass-based inks for building strong and bioactive scaffolds. However, despite the economic affordability, extrusion-based additive manufacturing methods suffer from the limitation of having ceramic or glass filaments as "structural units" of the scaffold that, thus, typically exhibits a grid-like architecture in 3D with parallel or strongly-oriented channels [71,84]. There is a general consensus on the fact that scaffolds closely mimicking the microarchitecture of the bone can promote osteogenic cell migration and reorganization as in the natural tissue, along with better osteointegration after implantation in vivo [85]. For this reason, it is highly desirable to produce bioceramic scaffolds having strong microarchitectural similarity to the bone tissue they have to replace. Section 5 will provide more details on how to assess this similarity. With regard to the fabrication strategy, the conventional method relying on foam replication is indeed highly effective and relatively simple for producing truly bone-like scaffolds [80]. It can be stated that additive manufacturing is preferable from the viewpoint of reliability and mechanical strength, while sponge replication is a unique technique from the viewpoint of bone-like biomimicry. In a recent paper, both methods – i.e. 3D printing and sponge replication – have been merged together to take the best from the two: specifically, a micro-computed tomography (micro-CT) reconstruction of a commercial open-cell polymeric foam was utilized as an input file to a vat photopolymerization system [67]. This fabrication approach was then extended to bioactive glass as well [68]. The whole manufacturing process is summarized in Fig. 4. It is

Table 2
Summary of the main fabrication techniques used for the production of bioactive glass and ceramic scaffolds for bone tissue engineering (data reported from selected studies).

Group of techniques	Technological class	Thermal consolidation (sintering)	Specific examples and references	Notes on porosity and mechanical properties
Conventional	Foaming techniques	Yes	H_2O_2 foaming of 45S5 glass [46]	Poorly interconnected pores
			Gel-casting foaming [55]	Porosity 75 vol%, compressive strengths of 3.4 ± 0.3 MPa, 8.4 ± 0.8 MPa and 15.3 ± 1.8 MPa, for ICIE16, PSrBG and 13–93 glass scaffolds, respectively
			Sol-gel foaming (only for bioactive glass scaffolds) [56,57]	70S30C glass scaffolds: porosity 78–88 vol%, compressive strength 0.3–4.5 MPa
	Starch consolidation	Yes	Starch from potato, corn or rice can be used [53]	Porosity range 23–70 vol%, compressive strength up to 6 MPa
	Space holder method (organic phase burn-off)	Yes	Natural porogen (e.g. rice husk) with 45S5 glass [50]	Porosity 45.9 ± 2.2 vol%, compressive strength: 7.2 ± 3.5 MPa
			Synthetic polymeric porogens (e.g. polyethylene particles) [51]	Porosity: 23.5–50.0 vol%; compressive strength: 20–150 MPa
	Porous polymer replication	Yes	Natural template (e.g. marine sponges) with 45S5 glass [58]	Porosity: 68–76 vol%; compressive strength: 1.8–4.0 MPa
			Synthetic foams (e.g. polyurethane foam) with various bioactive materials [59,60,61,62]	13-93 glass scaffolds: porosity: 85 vol%, compressive strength: 11 MPa; 45S5 glass scaffolds: porosity 65–92 vol%, compressive strength 0.2–2.5 MPa, SCNA glass scaffolds: porosity 56 ± 6 vol%, compressive strength 18 ± 5 MPa
	Freeze-drying	Yes	Freeze casting of suspensions [63]	Porosity 50 ± 4 vol%, compressive strength: 47 ± 5 MPa
	Thermally-induced phase separation	No	Composite scaffolds containing 45S5 glass [64]	Porosity >90 vol%, compressive modulus up to 26 MPa
	Solvent-casting and particulate leaching	No	Composite scaffolds containing 45S5 glass [65]	Porosity 94.05 ± 0.20 vol%, compressive strength: 0.07 ± 0.02 MPa
Additive manufacturing	Selective laser sintering	Yes	Bioactive glasses can be typically processed (e.g. 13–93 glass [66])	Porosity 55 ± 5 vol%, compressive strength: 20.4 ± 2.2 MPa
	Vat photopolymerization	Yes	Useful for both crystalline ceramics (e.g. hydroxyapatite [67] and glasses [68,69]. Digital light processing technique allows obtaining the best resolution among additive manufacturing techniques (few tens of micrometres)	Hydroxyapatite scaffolds: porosity ≈80 vol%, compressive strength 1.60 MPa; bioactive glass scaffolds: porosity up to 94 vol%, compressive strength up to 22 MPa
	Direct ink writing	Optional (fully inorganic or composite scaffolds can be obtained)	Variants of 3D printing, ink-jet printing, robocasting ([70,71,72,73])	SiO_2-based bioactive glass scaffolds: porosity 49.5 ± 5.5 vol%, compressive strength 6.1 ± 2.5 MPa; 13–93 bioactive glass: porosity 47 vol%, compressive strength 86 ± 9 MPa; MBG scaffolds: porosity 60.4 vol%, compressive strength 16.10 ± 1.53 MPa; 45S5 glass scaffolds: interconnected porosity 60–80 vol%, compressive strength 2–13 MPa.

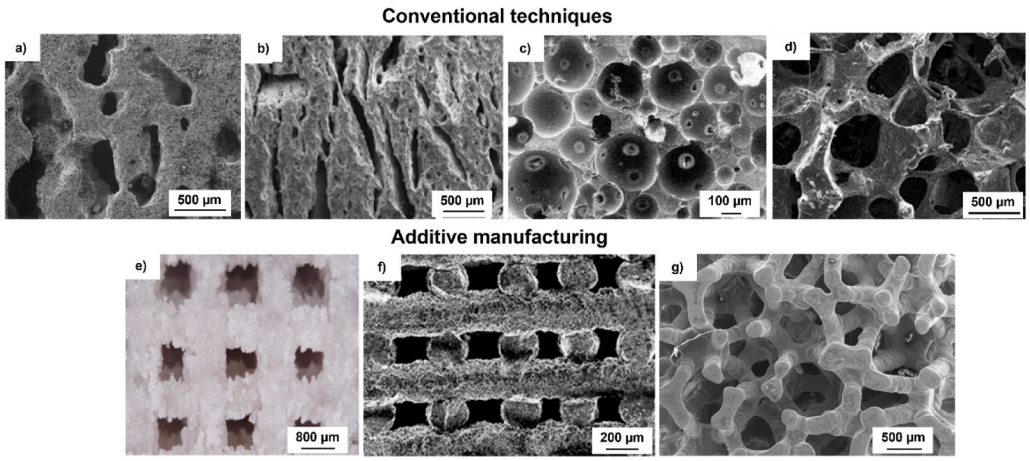

Fig. 3. Different types of bioactive ceramic and glass scaffolds produced by conventional or additive manufacturing technologies: (a) 45S5 Bioglass® scaffold using H_2O_2 foaming method (reproduced from Ref. [46]), (b) 45S5 Bioglass®-derived glass-ceramic scaffolds produced by rice husk burn-off (reproduced from Ref. [50]), (c) bioactive sol-gel glass foams (reproduced from Ref. [74]), (d) 45S5 Bioglass®-derived scaffold obtained by sponge replication (reproduced from Ref. [59]), (e) 13–93 bioactive glass scaffold made by selective laser sintering (reproduced from Ref. [66]), (f) robocasting of SiO_2-based bioactive glass scaffold (reproduced from Ref. [70]), (g) digital light processing stereolithography of hydroxyapatite scaffolds (reproduced from Ref. [67]).

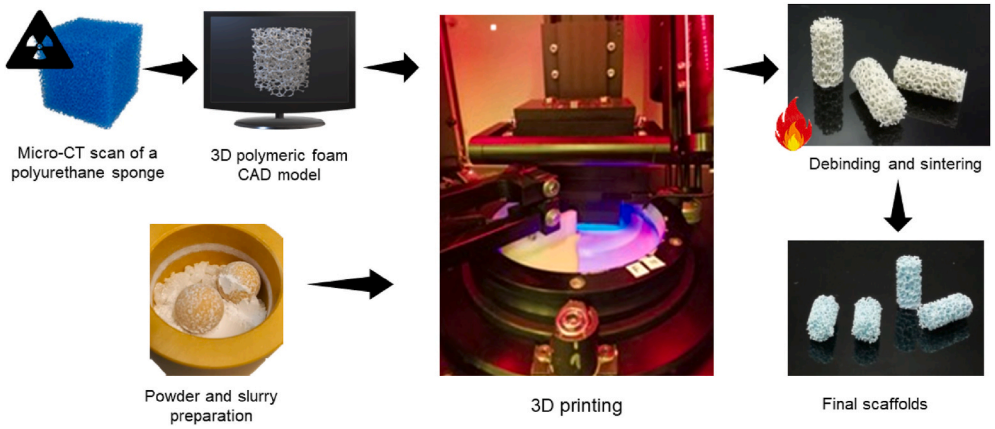

Fig. 4. Novel approach to fabricate bone-like scaffolds by additive manufacturing: the whole process involves the preparation of powders for the printable ink (bottom left), the creation of a foam-like "virtual" template by the micro-CT imaging of an open-cell commercial polyurethane sponge (top left), the printing operations by vat photopolymerization (centre), and the thermal treatment for debinding and sintering of the ceramic or glass scaffold (right).

worth highlighting that no medical images, e.g. coming from magnetic resonance scanning, are necessary in this approach, thus simplifying the procedure and overcoming any ethical issue related to the need for the patient's consensus. A certain degree of customization is also possible through a careful selection of the starting polymeric sponge: in fact, it is known that the total porosity and pore size of the final sintered product are dictated by the pores per inch (ppi) of the template, which is a commercial parameter reported on the technical datasheet of the polymer (the smaller the ppi, the higher the total pore volume and the larger the pore size) [86]. Therefore, using different foam reconstructions as CAD models to the printing system will yield scaffolds with different but controllable pore characteristics, which could mimic various types of bone.

4. Evaluation of scaffold suitability *a priori*: strategies for wise design and predictive approach

4.1. Architectural and mechanical properties

The predictive capability of mathematical or numerical models is crucial to achieve biomechanically effective devices, suitable implantation procedures and positive clinical outcomes. Material selection, biological response of cells, and the architectural design along with the permeability to fluid flow are simultaneously playing key roles in the design process of bioceramic scaffolds and should all be accounted for in the models to enable *a priori* evaluation of the devices.

The application of ceramic bone substitutes in load-bearing areas has been limited by the inherent brittleness of ceramic materials. Consequently, a critical requirement in designing bioceramic scaffolds is the ability to accurately predict their mechanical behaviour under physiological conditions. Since bone applications require highly porous micro-architected devices able to match mechanobiology constrains, the effective mechanical properties of the scaffolds are dramatically lower than the bulk material constituents. Both conventional and additive manufacturing technologies enable the creation of various micro-architectures, ranging from regular to random lattices (Fig. 5). Specifically, additive manufacturing technologies ideally allow for the fabrication of samples with exceptional geometric fidelity and prescribed porosity, pore size and trabecular (or wall) thickness. This high level of precision enhances the accuracy and usefulness of the corresponding numerical models [87]. Regular architectures yield higher possibilities of a fine geometrical control in the printing process and can be easily designed to achieve the target properties; on the other hand, they are typically optimized for specific loading scenarios [88].

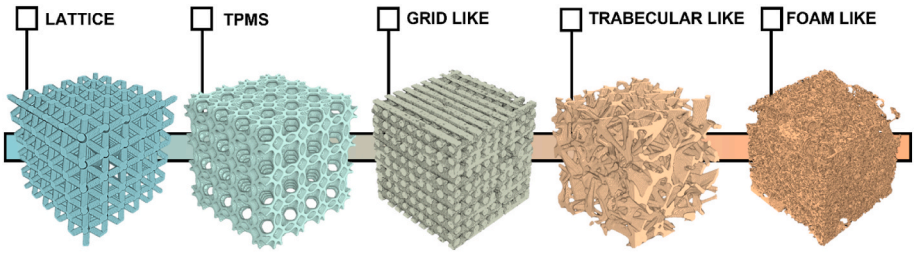

Fig. 5. Different design options for scaffolds, ranging from regular (periodic) to random geometries.

The porosity of the scaffolds (i.e. the ratio of void to total volume) has been considered for long time a key parameter to address the mechanobiology constraints, being relatively easy to control even with conventional manufacturing techniques. Thereby, several analytical models have been developed to relate such parameter to the effective stiffness and strength of the scaffolds, considering also the topologic arrangement of the structure, i.e. bending-dominated or stretching-dominated conditions [89]. Porosity is not the only morphological parameter that needs to be accounted for in determining the mechanical and biological response (see also section 5). In fact, the pore size and solid wall thickness play an even more significant role in the mechano-biological models, thus indicating that biological response and mechanics of the scaffolds need to be considered simultaneously in the design. Prediction of the mechanical response of each specific micro-structure can be achieved by means of Finite Element Models (FEM), being able to assess all the effective elastic constants of a scaffold, namely the effective Young's modulus, effective Poisson's coefficient and effective shear stiffness. These approaches date back to the early 1990s [90] and have widely been developed over the following decades, providing efficient tools in the scaffold design which are able to predict effective elastic properties as well as the full field of stress and strain. Another fundamental duty in scaffold design is the prediction of the effective strength: also in this case, FEM represents an efficient tool to predict the stress at failure of a device and the nucleation and evolution of the crack pattern that leads to the fracture [91,92]. It is worth noticing that sintered bioceramics show mechanical properties that are substantially dependent on the manufacturing process, such as the printing parameters and the conditions of the thermal treatments (e.g. debinding, sintering) applied to the green bodies [93]. Crystallization phenomena (which may happen concurrently to sintering in glasses, thus originating glass-ceramic materials), internal flaws and the characteristic size of the printed structure are all aspects that dictate the mechanical performances [94–96]. Consequently, in the early stages of technology development, numerical models require an experimental evaluation of the elastic modulus and strength of the ceramic material constituting the scaffold as they are qualities of a stochastic nature [97]. Once intrinsic material properties are available, micro-CT-based FEM can combine the architectural design of the scaffolds and the intrinsic defects related to manufacturing process, thus providing a good prediction of the effective strength [98–103]. Three representative examples are reported in Fig. 6 where fracture FEM have been used to predict the crack pattern under uniaxial compression in a triply-periodic minimal surface (TPMS) micro-architecture (in the left), in a bone-like scaffold (in the centre) and in a grid-like scaffold (in the right).

Although these models can be very accurate, their usage is dependent on the manufacturing of samples, micro-CT acquisitions and simulations through FEM that may result in expensive and time-consuming solutions. Optimization tools can be used to predict the effects of the manufacturing process, thus avoiding the production of the scaffolds and micro-CT scanning of the samples [105].

The mechanical strength of the bioactive ceramic scaffolds can be tuned within a wide range by appropriately designing the micro-architecture and by a suitable material selection. The scaffold strength can span from less than 10 MPa, which is enough to replace trabecular bone, to more than 100 MPa, which is more suitable for cortical bone replacement (see Fig. 7 adapted from Ref. [106]). A detailed review of the material-porosity-strength referred to a specific manufacturing technique (i.e. direct ink writing) is reported elsewhere [107].

Achieving an optimal compromise between strength and toughness is a challenging goal, as enhancing one property often compromises the other. A possible strategy to increase toughness is represented by the introduction of controlled distortions into the structure (like edge dislocation in metallic lattices), with a minimal trade-off in strength. This approach preserves other critical morphological parameters, such as porosity, wall spacing, and wall thickness, ensuring the material's overall integrity and consistency [108]. Other strategies to enhance the toughness of scaffolds include the application of polymeric coatings. While these coatings can effectively improve toughness, they may compromise the inherent high bioactivity of biomedical glasses and many ceramic materials [109].

Besides dictating the mechanical properties of the implant, porous architecture is also tightly related to permeability, which is another key parameter for the success of bone scaffolds. Mathematical and numerical models have been developed for the prediction of permeability [110]; it is worth mentioning that the permeability is independent of the material constituent of the solid phase of the scaffold and only the empty phase plays a role. Advanced analytical models can be used to predict the permeability considering also the tortuosity and the dimension of the

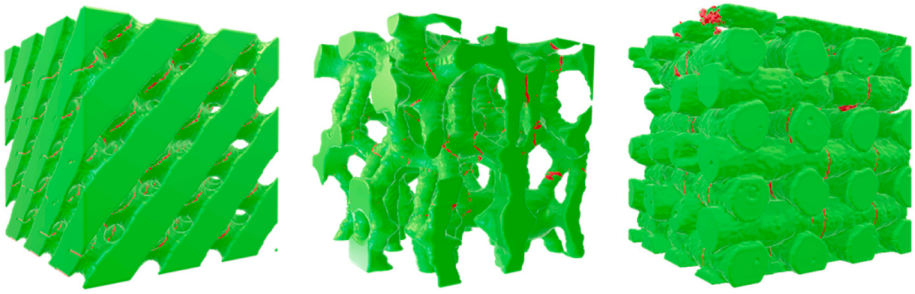

Fig. 6. Simulated crack pattern in different scaffolds upon compression (cracks are represented in red). The relevant finite element simulations are described in Refs. [100,102,104]. (For interpretation of the references to color in this figure legend, the reader is referred to the Web version of this article.)

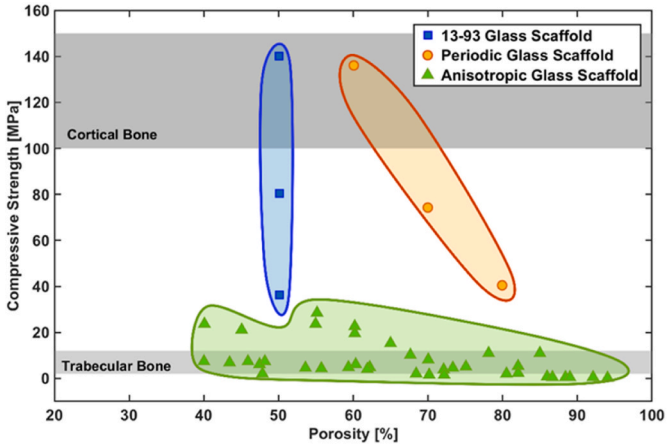

Fig. 7. Dependency of the compressive strength with respect to the porosity in glass and ceramic scaffolds (adapted from Ref. [89]).

pores (see also section 5) [9]. However, in order to gain specific information especially on intricated architectures, numerical simulations are often needed. Computational Fluid Dynamics (CFD) represent a powerful tool to get both effective properties and local phenomena. For instance, CFD simulations can predict both overall permeability of the device as well as local wall shear stress which is one of the factors affecting cell response [111–113].

4.2. Bone ingrowth and scaffold degradation

The mechanical properties of the scaffold indeed influence cell behavior and tissue regeneration. In this regard, suitable ranges of desirable mechanical properties are a prerequisite for tissue remodeling in order to avoid the adverse consequences of stress-shielding (adaptive changes in bone strength and stiffness) occurring due to the difference in the properties of the bone and the implant material (see also section 2).

The success of scaffolding procedure is related to the ability of native bone tissue to colonize the scaffold. The cellular growth has been modeled initially by coupling two phenomena, namely the local deformation of the scaffold under a loading condition and the wall shear stress of the fluid flowing on the walls of the scaffold. Coupled with experimental observations, the mechanical stimulus can be defined and used to predict bone resorption as well as bone cell proliferation or differentiation [114]. However, this model is able to predict only the early stage of the cell behavior as the in vivo environment is a dynamic system and more complex models are needed for suitable prediction purposes. Agent Based Models (ABM) can be employed to study how individual bone cells interact with each other and their environment to contribute to bone growth, remodeling, and repair [115]. Also, the local curvature of the scaffold affects the cell behavior [116]: specifically, walls with at least one negative principal curvature have been found to be beneficial for bone cell proliferation [117]. Mechanobiological models that consider parameters such as the concentrations of osteogenic growth factors, cell activities (e.g. migration and apoptosis), oxygen concentration and angiogenesis, confirm that high negative curvatures (concave surfaces) promote the deposition of new bone [118].

Thanks to the bioactivity of glass and many ceramic scaffolds, bone growth begins almost immediately following implantation, leading to significant improvements in both the stiffness and strength of the device. Therefore, the prediction of the stiffness and the strength must be intended at the time of the implantation. The rapid osseointegration results in a composite structure where the ceramic scaffold is closely coupled with newly-formed bone. The latter effectively acts as a toughening agent, distributing stress more evenly and preventing crack propagation [119]. On the other hand, also the degradation of the scaffolds occurs, and it can be modeled and predicted, too [120].

4.3. The potential of Artificial Intelligence applied to scaffold design

The evolution of numerical simulations for the prediction of the overall response of a scaffold allowed the development of multidisciplinary optimization algorithms for personalized bone-substitute implants. Modern additive manufacturing methods, such as vat photopolymerization, provide a plethora of options for the architectural arrangement of microstructural components and their spatial variation in the osseous defect to be treated. Together with design variables related to material properties (e.g. volumetric proportions of amorphous and crystalline phases in glass-ceramics), architectural features define a very large design space (meaning the set of possible designs that can be produced), making the design process difficult and time-consuming. The optimal design is achieved by means of multidisciplinary objectives, e.g. (i) maximizing implant strength, (ii) minimizing elastic mismatch and stress shielding or stress concentration in the receiving bone, (iii) improving flow properties for adequate cell nutrient transport and waste disposal through the microstructure and (iv) maximizing tissue growth and growth rates. Some representative examples of personalized optimal design are reported in Refs. [121–123]. The application of Artificial Intelligence (AI) in the design of bone scaffolds has been growing in recent years, due to the proven effectiveness of this type of techniques in processing large amount of data, often heterogeneous by nature, achieved in other fields (e.g. Computer Vision). The scaffold design process indeed involves generation of data at different levels of the pipeline. For example, the design of the geometrical model of the scaffold usually requires a dataset of images collected through micro-CT scanning or magnetic resonance, then complex algorithms are executed for segmenting the tissue [124], reconstructing the volume [125], and finally producing the blueprint for 3D printing [90]. It is possible to conceptualize multidisciplinary optimization tasks by utilizing AI approaches such as machine learning techniques. These can be formulated for the identification of an optimal scaffold design based on TPMS topologies exhibiting prescribed mechanical, physical or morphometric target properties [104]. Extensive data, which may be generated through numerical models or measured in laboratory experiments, must be used to train the techniques. As an example of these generated data, Fig. 8 shows the trend of morphologic features and mechanical properties for hydroxyapatite scaffolds belonging to two classes of TPMS (diamond and gyroid). In particular, wall thickness, pore size, effective pore connectivity index (which is an indirect indicator of the fluid permeability [126]) and an index of strength [127] are reported. In Fig. 8 panel (a) the optimal range on the wall thickness determined by the manufacturing technology of ceramic scaffolds (the vat photopolymerization, in this case) is shown; furthermore, the range of pore size for optimal biological response is also shown. The colors of the datapoints are proportional to the strength index (cold colors refer to weaker scaffolds). Fig. 8 panel (b) shows similar information but considering the pore spacing: it shows how larger pores may guarantee higher fluid permeability but lower mechanical strength; therefore, optimization strategies are needed to identify trade-off solutions. Traditional design approaches often fall short in adequately addressing these complexities. Consequently, the application of AI techniques allows analyzing vast datasets to identify patterns and relationships among different microstructural and mechanical features that are not readily apparent through conventional methods. This capability allows for the development of scaffolds that meet specific biomechanical requirements more precisely [128,129].

In future applications, mathematical and numerical models will play a crucial role in the effective design of scaffolds, especially when dealing with complex geometries. These models enable the customization of scaffold designs that are tailored to the specific needs of individual patients, moving beyond the limitations of off-the-shelf devices. By incorporating patient-specific data, such as anthropometric parameters,

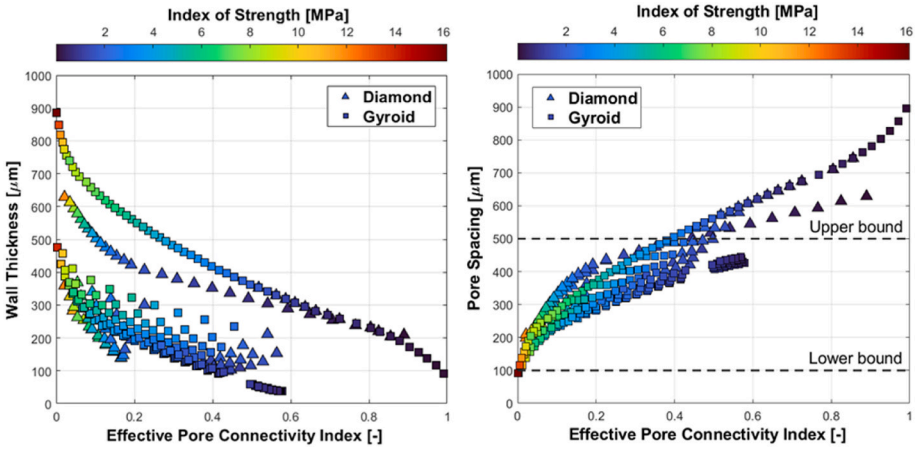

Fig. 8. Trends of morphological and mechanical properties of TPMS hydroxyapatite scaffolds (original data available in the study presented in Ref. [104]).

these models would allow for the simulation of scaffold performance under realistic loading conditions, which is critical for predicting the mechanical behavior and overall effectiveness of the scaffold in a clinical setting. To this aim, topologic optimization represents a useful design tool able to match the anatomy of the patient and optimize the microstructure according to the load conditions [130]. This personalized approach ensures that the scaffolds are optimized for each patient, improving outcomes and enhancing the integration of the scaffold with the surrounding tissue.

5. Evaluation of scaffold suitability *a posteriori*

After being produced and prior to being used, the scaffold has to be characterized to reliably assess its characteristics and, hence, its suitability for bone applications. In other words, it is necessary to check the matching between scaffold properties (mainly architectural characteristics but also (bio)mechanical aspects) and the ideal requirements that an "optimal" scaffold should fulfil. As discussed in section 2, a number of basic requirements have been identified, ranging from biocompatibility (which can be checked by in vitro tests with cells) to pore features. With regard to the pore network, typical "acceptance criteria" include total porosity above 50 vol%, pore sizes in the range of 100–500 μm, and high interconnectivity of the pores [33]. Mechanical properties, which are tightly dependent both on the inherent characteristics of the material and on the pore/strut arrangement of the scaffold in 3D, are also considered; a couple of parameters that are commonly assessed include elastic modulus (0.05–0.5 GPa) and compressive strength (which is recommended to be above 1–2 MPa) [131]. These reference values for structural and mechanical properties come from those of healthy human cancellous bone [132,133] and the ranges for the different parameters may be quite broad.

Total porosity and average pore diameter (under the assumption that pores are approximated as spherical ones) are relatively easy to determine by mass-volume gravimetric measurements and SEM/micro-CT, respectively; therefore, they are still commonly used as the key parameters to quantitatively assess the "goodness" of scaffolds for bone applications or to compare different scaffold types. Pore interconnectivity is often analyzed from a qualitative viewpoint (e.g. permeation of a colored fluid through the pores [52]), unless a micro-CT equipment is available for proper quantification [134]. However, knowing only total porosity and mean pore size cannot describe properly the 3D structure of a macroporous scaffold and, hence, its similarity to cancellous bone; therefore, also the relevant predictions about bone-regenerative capability based only on these parameters may be markedly incomplete. These limitations were well underlined by Hollister et al. [135] who reported no statistically significant difference with regard to regenerated bone volume within poly(propylene fumarate)/TCP composite scaffolds having total porosity of 30, 50 or 70 vol%: this finding apparently contradicts the idea that the higher the porosity, the better the bone ingrowth. Roosa et al. [136] also observed that different pore sizes in the range of 350–800 μm within polycaprolactone scaffolds had a very poor impact on bone regeneration rate. These findings reveal the complexity and interdependency of scaffold microstructural features and their mutual effect on the bone regeneration process along with the key role that is inherently played by the scaffold material (e.g. inert polymer vs. osteoinductive TCP) [137]; this last issue, however, is not discussed in the present contribution and the reader interested in the search for chemically bone-like biomaterials is addressed to specific publications on this topic [138,139].

5.1. Towards a scaffold-to-bone similarity score

In order to obtain a more comprehensive quantification of the "goodness" of scaffolds in terms of bone similarity, the use of a multiparametric score accounting for a combination of six microstructural independent parameters was proposed, i.e. total porosity, pore interconnectivity, pore size distribution, specific surface area, connectivity density and degree of anisotropy [140]. This microarchitectural bone similarity score (BOSS) was defined as the squared distance between the samples – either bioceramic scaffolds vs. trabecular bone or pairs of different scaffolds to be compared – in the multi-dimensional space of the parameters considered above and, according to this definition, the smaller the BOSS, the more similar the two samples. An extension of this approach was also proposed by the same research group to take into account two additional mechanical properties, specifically elastic modulus and compressive strength, in the same score that actually became a microarchitectural/biomechanical BOSS [141]. Fig. 9 summarizes the philosophy behind the concept of BOSS and its physico-mathematical definition; the dissimilarity index associated to the comparison of pore size distributions was defined according to White [142], and the weighting coefficients for the different parameters were estimated in Ref. [143]. It is worth highlighting that the BOSS scoring system potentially allows great customization in terms of scaffold design or selection, which can be truly guided by the properties of the targeted bone tissue (i.e., in other words, by the clinical requirements). Therefore, the variability in bone tissue properties is accounted in the BOSS, which would become a comparative tool available to doctors for selecting the "best" implant for a given patient as well as to manufacturers to tailor the scaffold properties depending on the specific clinical requirements (personalized medicine). In order to demonstrate the versatility of this scoring system, a conceptually-analogous similarity index was also proposed for other applications than bone tissue engineering (i.e., porous ceramics for ocular applications [144]).

Such an approach, although potentially being very powerful, suffers

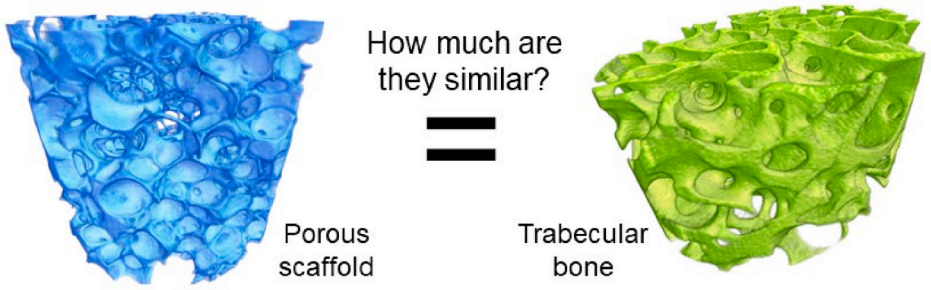

EIGHT PARAMETERS (microstructural + mechanical properties):

- Total porosity, ε
- Interconnectivity index, I_p (fraction of the void volume accessible from the outside)
- Pore size distribution, $f(d_p)$
- Specific surface area, a_v
- Connectivity index, β (quantification of strut connections)
- Degree of anisotropy, DA (measure of the preferential alignment of solid struts along particular directions)

→ Micro-CT

- Elastic modulus, E
- Compressive strength, σ_c

→ Compressive test (destructive)

DEFINITION OF THE SIMILARITY SCORE:

$$d_{i,h-k,raw} = |p_{i,h} - p_{i,k}|$$

absolute difference (distance) of the i-th mean property value p_i between the h-th and the k-th sample

$$d_{i,h-k} = w_i \frac{|p_{i,h} - p_{i,k}|}{s_i}$$

rescaling (with respect to the experimental standard deviation s_i of that feature estimated from the measurements performed on all samples) and weighing (coefficients w_i)

Only for the pore size distribution a dissimilarity index was defined:

$$d_{i,h-k}\left(f(d_{p,h})\ vs.\ f(d_{p,k})\right) = \frac{1}{2}\sum_{j=1}^{N}|n_{j,h} - n_{j,k}|$$

$d_{p,h}$ and $d_{p,k}$ are the middle values of the pore size classes of the h-th and k-th sample
$n_{j,h}$ and $n_{j,k}$ are the percent pore number within the j-th class of the h-th and k-th sample
N is the number of the pore size classes

$$\boldsymbol{BOSS} = \sum_{i=1}^{8} \boldsymbol{d_{i,h-k}^2}$$

squared distance (*quadrance*) between the samples in the eight-dimensional space of the considered features

Fig. 9. Scope, definition and mathematical calculation of the BOSS.

from two main limitations. The first issue concerns the number and types of scaffold properties to be considered in the calculation of BOSS. The six microarchitectural parameters used in both studies [140] were selected being supposed to be independent of other properties and, based on the literature, as highly representative to describe the bone-scaffold similarity; however, new properties could be added. A systematic study of all measurable properties of scaffolds and bone tissues harvested from different anatomical sites of humans varying by sex and age would allow gaining more information on how these parameters are independent to one another and would help defining a BOSS threshold below which a scaffold has to be considered truly similar to a given bone tissue. This opens a crucial question: what are the boundaries of BOSS? In fact, many additional independent properties also dealing, for example, with the biological properties of the scaffold material (e.g. biocompatibility and bioactivity) and the scaffold dissolution rate, which can modify the pore characteristics and hence the scaffold architecture over time, could be potentially included in the BOSS. The second problem of the BOSS as defined in Refs. [140,141] concerns the weights to be assigned to the different parameters in the calculation of the score (see Fig. 9): the value of BOSS, even if referred to the same pair of samples, can thus slightly vary depending on the weighing coefficients and is valid only for comparative purposes under the same assumptions. Making use of large datasets could help in this regard, and machine learning-assisted studies would deserve to be conducted in the future to better understand the potential and real applicability of this score.

5.2. Permeability: a comprehensive architectural parameter

If we want to focus on the porous network of the scaffold and bypass the path of BOSS assessment, a "global" descriptive parameter is represented by the intrinsic permeability, which also dictates the mass transport properties that are tightly related to bone growth and regeneration. In general, permeability quantifies the ability of a porous material to conduct fluid flow and inherently depends on a combination of open porosity, pore size, pore orientation, tortuosity and interconnectivity [145]. It should be highlighted that permeability provides a much more significant and robust information (also relevant to biological performance) compared to total porosity, which includes closed and isolated pores, too, that do not allow fluid to flow or living cells to colonize the porous device. Therefore, a simple acceptance criterion for scaffold could be the following: the closer the scaffold permeability to bone permeability, the more bone-like (and more functional) the scaffold.

The significance of permeability in the framework of bioceramic scaffold development and selection has also been comprehensively discussed in Ref. [146].

The permeability of bioactive glass and ceramic foams can be assessed either by numerically solving the Stokes equations relevant to the system geometry [147] or experimentally by implementing the Darcy's law (under laminar flows) and using a fluid (typically water) as permeation medium through the scaffold [148]. A specific ASTM standard describes the procedure to perform for assessing the permeability of tissue engineering scaffolds using a fluid flowing through the 3D porous structure under a pressure gradient [149]. However, this approach requires the use of three transducers to assess upstream and downstream pressures and flow rate and may be not advisable for very delicate or resorbable scaffolds, like bioactive glass or ceramic foams with thin struts, which might be damaged by the fluid flow during the execution of the measurement. A smart strategy has been recently proposed to determine the intrinsic permeability of hydroxyapatite [150] and bioactive glass scaffolds [151] by measuring the pressure wave drop of a slow alternating airflow, provided that the volumetric airflow rate through the scaffold is known. In this way, only one single transducer – i.e. a microphone – is necessary. The value of permeability experimentally measured by this non-destructive acoustic method can then be used to assess the complete set of mass transport properties of – potentially – any kind of bioceramic scaffolds by combining the concepts from Ergun-Wu resistance model [152] with appropriate physical modelling of the scaffold structure/porous network and reliable data from advanced 3D imaging (e.g. micro-CT).

6. Conclusions and outlook

Conventional methods and additive manufacturing technologies offer plenty of possibilities to fabricate porous ceramic and glass scaffolds as well as polymer-matrix composites embedding bioactive inorganic inclusions. From the viewpoint of processing – including versatility aspects (e.g. fabrication of structures with complex shapes), accuracy of manufacturing, scalability of results and overall quality of the final product –, vat photopolymerization shows great promise [153]. This technology is highly appealing because it can reach the best achievable resolution (below 40 μm) among the currently-available CAD-CAM printing methodologies for ceramic materials, even when implemented at the industrial level for mass production. On the contrary, conventional burn-off methods – which are conceptually simple but yield bioceramic scaffolds with predominantly closed and isolated macropores – are not the ideal ones to produce truly bone-like structures.

Indeed, before 3D printed bioceramic bone substitutes gain confidence among the main stakeholders they need to achieve a degree of confidence and a quality level which must be comparable to that of traditional implants. Hence, new design solutions using computational models and efficient manufacturing processes capable of ensuring high printing fidelity are key to accomplish the goal.

With regard to the optimal 3D porous architecture, the question still remains open and, at present, one cannot state that a porous arrangement of open pores is definitely superior in stimulating bone regeneration compared to another configuration. An interesting comparison was reported in a study by Liu et al. [77], who implanted 13–93 bioactive glass scaffolds with either oriented pores or a foam-like structure in rat calvaria defects: after 12 postoperative weeks, trabecular scaffolds showed better integration with host bone compared to the columnar counterparts, but after 24 weeks an inversion of this trend was noted with more bone in-growth in the scaffolds with parallel channels. The tortuosity of pores in the glass foam might have played a role in making the diffusion of nutrient and oxygen as well as the vascularization more difficult compared to the other scaffold type, thus inhibiting new bone formation over time.

TPMS geometries, which exhibit minimal area, full interconnectivity of pores/channels and zero-mean curvature [154], also show great promise and deserve further investigation in the future. In fact, it was shown that cancellous bone has similar properties to TPMS structures [155]. However, a limiting factor in producing TPMS scaffolds is that they can be obtained only by additive manufacturing technologies. Future studies should be addressed on understanding the actual influence of the different scaffold micro- and macro-architectures on cells, i.e., in other words, how cells "sense" different (macro)pore orientation and arrangement in 3D, in order to truly design optimal scaffolds from both structural and biological viewpoints. To date, relevant studies are quite scarce in the literature. Surprisingly, no statistically different results were reported for in vitro cell experiments (pre-osteoblastic murine cells) on calcium phosphate scaffolds with conventional grid-like or Kagome lattice architectures [156], suggesting that more refined studies have to be planned and performed in the future to gain more knowledge on these aspects. In this regard, an issue deserving further investigation is the role played by local geometrical features of the scaffold, like curvature, on tissue growth and regeneration [157,158].

Once the scaffold has been fabricated, a key issue concerns the reliable evaluation of implant suitability for bone repair. Plenty of aspects, ranging from architectural features to biomechanical properties and cell interactions, should ideally be considered to provide a convincing response. Machine learning methods are expected to play an

increasing role in the management and analysis of such large amounts of data to aid scientist in the decision-making process. Alternatively, if we use an apparently more "reserved" approach and focus on the micro-architecture, intrinsic permeability can indeed be assumed as a global parameter accounting for a number of pore-related characteristics. Furthermore, permeability is tightly related to mass transport properties, which in turn dictate the biological performance of scaffold in vivo. Knowing the permeability, important microstructural parameters can be estimated for quantitative assessment and comparison like tortuosity, which also plays a role from a biomechanical viewpoint (the mechanical strength of trabecular structures increases as tortuosity decreases [159]). A possible drawback is related to the experimental assessment of permeability, which typically requires a dedicated equipment that needs to be purposely adapted depending on sample shape and size, and should be corroborated by a robust statistical analysis of acquired data [150].

CRediT authorship contribution statement

Francesco Baino: Writing – review & editing, Writing – original draft, Supervision, Project administration, Methodology, Investigation, Funding acquisition, Conceptualization. **Roberta Gabrieli:** Writing – review & editing, Writing – original draft, Methodology, Investigation, Conceptualization. **Enrica Verné:** Writing – review & editing, Supervision, Methodology, Conceptualization. **Alessandro Schiavi:** Writing – review & editing, Methodology, Conceptualization. **Martin Schwentenwein:** Writing – review & editing, Methodology, Conceptualization. **Luca D'Andrea:** Writing – review & editing, Writing – original draft, Methodology, Investigation, Conceptualization. **Pasquale Vena:** Writing – review & editing, Writing – original draft, Supervision, Project administration, Methodology, Investigation, Funding acquisition, Conceptualization.

Declaration of competing interest

The authors declare that they have no known competing financial interests or personal relationships that could have appeared to influence the work reported in this paper.

Acknowledgements

This study was carried out within the project "Artificial Intelligence-based design of 3D PRINTed scaffolds for the repair of critical-sized BONE defects - I-PRINT-MY-BONE" funded by European Union – Next Generation EU within the PRIN 2022 program (D.D. 104 - February 02, 2022 Ministero dell'Università e della Ricerca). This manuscript reflects only the authors' views and opinions and the Ministry cannot be considered responsible for them.

Appendix A. Supplementary data

Supplementary data to this article can be found online at https://doi.org/10.1016/j.ceramint.2025.02.307.

References

[1] J.F. Keating, A.H.R.W. Simpson, C.M. Robinson, The management of fractures with bone loss, J Bone Joint Surg Br 87-B (2) (2005) 142–150, https://doi.org/10.1302/0301-620X.87B2.15874.
[2] P. V Giannoudis, H. Dinopoulos, E. Tsiridis, Bone substitutes: an update, Injury 36 (3) (Nov. 2005) S20–S27, https://doi.org/10.1016/j.injury.2005.07.029.
[3] E.E. Huang, et al., Novel techniques and future perspective for investigating critical-size bone defects, Bioengineering 9 (4) (2022), https://doi.org/10.3390/bioengineering9040171.
[4] G. Brunello, S. Panda, L. Schiavon, S. Sivolella, L. Biasetto, M. Del Fabbro, The impact of bioceramic scaffolds on bone regeneration in preclinical in vivo studies: a systematic review, Materials 13 (7) (2020), https://doi.org/10.3390/ma13071500.
[5] N. Reznikov, R. Shahar, S. Weiner, Bone hierarchical structure in three dimensions, Acta Biomater. 10 (9) (2014) 3815–3826, https://doi.org/10.1016/j.actbio.2014.05.024.
[6] M.P. Nikolova, M.S. Chavali, Recent advances in biomaterials for 3D scaffolds: a review, Bioact. Mater. 4 (2019) 271–292, https://doi.org/10.1016/j.bioactmat.2019.10.005.
[7] L. Hench, D. Greenspan, Interactions between bioactive glass and collagen: a review and new perspectives, Journal of the Australian Ceramic Society 49 (Jan. 2013) 1–40.
[8] D. Greenspan, Bioglass at 50 – a look at Larry Hench's legacy and bioactive materials 5 (1) (2019) 178–184, https://doi.org/10.1515/bglass-2019-0014.
[9] E. Fiume, A. Schiavi, G. Orlygsson, C. Bignardi, E. Verné, F. Baino, Comprehensive assessment of bioactive glass and glass-ceramic scaffold permeability: experimental measurements by pressure wave drop, modelling and computed tomography-based analysis, Acta Biomater. 119 (2021) 405–418, https://doi.org/10.1016/j.actbio.2020.10.027.
[10] S.V. Dorozhkin, Calcium Orthophosphates as Bioceramics: State of the Art, MDPI AG, Nov. 30, 2010, https://doi.org/10.3390/jfb1010022.
[11] L.C. Gerhardt, A.R. Boccaccini, Bioactive glass and glass-ceramic scaffolds for bone tissue engineering, Materials 3 (7) (2010) 3867–3910, https://doi.org/10.3390/ma3073867.
[12] F. Baino, et al., Processing methods for making porous bioactive glass-based scaffolds—a state-of-the-art review, Int. J. Appl. Ceram. Technol. 16 (5) (Sep. 2019) 1762–1796, https://doi.org/10.1111/ijac.13195.
[13] A. Hoppe, N.S. Güldal, A.R. Boccaccini, A review of the biological response to ionic dissolution products from bioactive glasses and glass-ceramics, Biomaterials 32 (11) (2011) 2757–2774, https://doi.org/10.1016/j.biomaterials.2011.01.004.
[14] F. Baino, Ceramics for bone replacement, in: Advances in Ceramic Biomaterials, 2017, pp. 249–278, https://doi.org/10.1016/B978-0-08-100881-2.00007-5.
[15] M.A. Sainz, S. Serena, M. Belmonte, P. Miranzo, M.I. Osendi, Protein adsorption and in vitro behavior of additively manufactured 3D-silicon nitride scaffolds intended for bone tissue engineering, Mater. Sci. Eng. C 115 (2020) 110734, https://doi.org/10.1016/j.msec.2020.110734.
[16] C.M. Paione, F. Baino, Non-Oxide Ceramics for Bone Implant Application: State-Of-The-Art Overview with an Emphasis on the Acetabular Cup of Hip Joint Prosthesis, MDPI, Jun. 01, 2023, https://doi.org/10.3390/ceramics6020059.
[17] S. Sadeghzade, et al., Recent advances on bioactive baghdadite ceramic for bone tissue engineering applications: 20 years of research and innovation (a review), Mater Today Bio 17 (2022) 100473, https://doi.org/10.1016/j.mtbio.2022.100473.
[18] V. Campana, et al., Bone substitutes in orthopaedic surgery: from basic science to clinical practice, J. Mater. Sci. Mater. Med. 25 (10) (Sep. 2014) 2445–2461, https://doi.org/10.1007/s10856-014-5240-2.
[19] T. Albrektsson, C. Johansson, Osteoinduction, osteoconduction and osseointegration, Eur. Spine J. 10 (2001) S96–S101, https://doi.org/10.1007/s005860100282.
[20] M.M. Stevens, Biomaterials for bone tissue engineering, Mater. Today 11 (5) (2008) 18–25, https://doi.org/10.1016/S1369-7021(08)70086-5.
[21] W. Cao, L.L. Hench, Bioactive materials, Ceram. Int. 22 (6) (1996) 493–507, https://doi.org/10.1016/0272-8842(95)00126-3.
[22] D.S. Brauer, Bioactive glasses—structure and properties, Angew. Chem. Int. Ed. 54 (14) (Mar. 2015) 4160–4181, https://doi.org/10.1002/anie.201405310.
[23] N. Eliaz, N. Metoki, Calcium phosphate bioceramics: a review of their history, structure, properties, coating technologies and biomedical applications, Materials 10 (4) (2017), https://doi.org/10.3390/ma10040334.
[24] I. Ielo, G. Calabrese, G. De Luca, S. Conoci, Recent advances in hydroxyapatite-based biocomposites for bone tissue regeneration in orthopedics, Int. J. Mol. Sci. 23 (17) (2022), https://doi.org/10.3390/ijms23179721.
[25] C. Dong, G. Tan, G. Zhang, W. Lin, G. Wang, The Function of Immunomodulation and Biomaterials for Scaffold in the Process of Bone Defect Repair: A Review, Frontiers Media S.A, 2023, https://doi.org/10.3389/fbioe.2023.1133995.
[26] Z. Sheikh, S. Najeeb, Z. Khurshid, V. Verma, H. Rashid, M. Glogauer, Biodegradable Materials for Bone Repair and Tissue Engineering Applications, MDPI AG, 2015, https://doi.org/10.3390/ma8095273.
[27] R. Gruber, H. Koch, B.A. Doll, F. Tegtmeier, T.A. Einhorn, J.O. Hollinger, Fracture healing in the elderly patient, Exp. Gerontol. 41 (11) (2006) 1080–1093, https://doi.org/10.1016/j.exger.2006.09.008.
[28] A.A. El-Rashidy, J.A. Roether, L. Harhaus, U. Kneser, A.R. Boccaccini, Regenerating bone with bioactive glass scaffolds: a review of in vivo studies in bone defect models, Acta Biomater. 62 (2017) 1–28, https://doi.org/10.1016/j.actbio.2017.08.030.
[29] T.M. Keaveny, E.F. Morgan, G.L. Niebur, O.C. Yeh, Biomechanics of trabecular bone, Annu. Rev. Biomed. Eng. 3 (3) (2001) 307–333, https://doi.org/10.1146/annurev.bioeng.3.1.307, 2001.
[30] I.D. Thompson, L.L. Hench, Mechanical properties of bioactive glasses, glass-ceramics and composites, Proc. Inst. Mech. Eng. H 212 (2) (1998) 127–136, https://doi.org/10.1243/0954411981533908.
[31] F. Javed, H. Ahmed, R. Crespi, G. Romanos, Role of Primary Stability for Successful Osseointegration of Dental Implants: Factors of Influence and Evaluation, Akademiai Kiado Zrt, Dec. 01, 2013, https://doi.org/10.1556/IMAS.5.2013.4.3.
[32] C. Turner, M. Forwood, M. Otter, Mechanotransduction in bone: do bone cells act as sensors of fluid flow? FASEB J. 8 (Sep. 1994) 875–878, https://doi.org/10.1096/fasebj.8.11.8070637.

[33] V. Karageorgiou, D. Kaplan, Porosity of 3D biomaterial scaffolds and osteogenesis, Biomaterials 26 (27) (2005) 5474–5491, https://doi.org/10.1016/j.biomaterials.2005.02.002.
[34] S.F. Hulbert, F.A. Young, R.S. Mathews, J.J. Klawitter, C.D. Talbert, F.H. Stelling, Potential of ceramic materials as permanently implantable skeletal prostheses, J. Biomed. Mater. Res. 4 (3) (Sep. 1970) 433–456, https://doi.org/10.1002/jbm.820040309.
[35] A. Szczodra, et al., Impact of borosilicate bioactive glass scaffold processing and reactivity on in-vitro dissolution properties, Mater. Today Commun. 35 (2023) 105984, https://doi.org/10.1016/j.mtcomm.2023.105984.
[36] A.R. Amini, C.T. Laurencin, S.P. Nukavarapu, Bone Tissue Engineering: Recent Advances and Challenges, 2012.
[37] A.G. Abdelaziz, et al., A Review of 3D Polymeric Scaffolds for Bone Tissue Engineering: Principles, Fabrication Techniques, Immunomodulatory Roles, and Challenges, MDPI, Feb. 01, 2023, https://doi.org/10.3390/bioengineering10020204.
[38] S.S. Lee, X. Du, I. Kim, S.J. Ferguson, Scaffolds for bone-tissue engineering, Matter 5 (9) (2022) 2722–2759, https://doi.org/10.1016/j.matt.2022.06.003.
[39] B. Feng, et al., The effect of pore size on tissue ingrowth and neovascularization in porous bioceramics of controlled architecture in vivo, Biomed. Mater. 6 (1) (2011) 015007, https://doi.org/10.1088/1748-6041/6/1/015007.
[40] C. Ghayor, F.E. Weber, Osteoconductive microarchitecture of bone substitutes for bone regeneration revisited, Front. Physiol. 9 (JUL) (Jul. 2018), https://doi.org/10.3389/fphys.2018.00960.
[41] M. Alonzo, et al., Bone Tissue Engineering Techniques, Advances, and Scaffolds for Treatment of Bone Defects, Elsevier B.V., Mar. 01, 2021, https://doi.org/10.1016/j.cobme.2020.100248.
[42] T.M. Koushik, C.M. Miller, E. Antunes, Bone tissue engineering scaffolds: function of multi-material hierarchically structured scaffolds, Adv. Healthcare Mater. 12 (9) (Apr. 2023) 2202766, https://doi.org/10.1002/adhm.202202766.
[43] K. Anselme, P. Davidson, A.M. Popa, M. Giazzon, M. Liley, L. Ploux, The interaction of cells and bacteria with surfaces structured at the nanometre scale, Acta Biomater. 6 (10) (2010) 3824–3846, https://doi.org/10.1016/j.actbio.2010.04.001.
[44] M.J. Grimm, J.L. Williams, Measurements of permeability in human calcaneal trabecular bone, J. Biomech. 30 (7) (1997) 743–745, https://doi.org/10.1016/S0021-9290(97)00016-X.
[45] A. Syahrom, M.R. Abdul Kadir, J. Abdullah, A. Öchsner, Permeability studies of artificial and natural cancellous bone structures, Med. Eng. Phys. 35 (6) (2013) 792–799, https://doi.org/10.1016/j.medengphy.2012.08.011.
[46] H. Yuan, J.D. De Bruijn, X. Zhang, C.A. Van Blitterswijk, K. De Groot, Bone induction by porous glass ceramic made from Bioglass® (45S5), J. Biomed. Mater. Res. 58 (3) (2001) 270–276, https://doi.org/10.1002/1097-4636(2001)58:3<270::AID-JBM1016>3.0.CO;2-2.
[47] Q. Fu, E. Saiz, M.N. Rahaman, A.P. Tomsia, Bioactive glass scaffolds for bone tissue engineering: state of the art and future perspectives, Mater. Sci. Eng. C 31 (7) (2011) 1245–1256, https://doi.org/10.1016/j.msec.2011.04.022.
[48] F. Baino, G. Novajra, C. Vitale-Brovarone, Bioceramics and Scaffolds: A Winning Combination for Tissue Engineering, Frontiers Media S.A, 2015, https://doi.org/10.3389/fbioe.2015.00202.
[49] F. Baino, M. Ferraris, Learning from Nature: using bioinspired approaches and natural materials to make porous bioceramics, Int. J. Appl. Ceram. Technol. 14 (4) (Jul. 2017) 507–520, https://doi.org/10.1111/ijac.12677.
[50] S.C. Wu, H.C. Hsu, S.H. Hsiao, W.F. Ho, Preparation of porous 45S5 Bioglass®-derived glass-ceramic scaffolds by using rice husk as a porogen additive, J. Mater. Sci. Mater. Med. 20 (6) (Jun. 2009) 1229–1236, https://doi.org/10.1007/s10856-009-3690-8.
[51] F. Baino, E. Verné, C. Vitale-Brovarone, 3-D high-strength glass-ceramic scaffolds containing fluoroapatite for load-bearing bone portions replacement, Mater. Sci. Eng. C 29 (6) (Aug. 2009) 2055–2062, https://doi.org/10.1016/j.msec.2009.04.002.
[52] D. Bellucci, V. Cannillo, A. Sola, C. Federica, M. Gazzarri, C. Migone, Macroporous bioglass®-derived scaffolds for bone tissue regeneration, Ceramics International - CERAM INT 37 (Jul. 2011) 1575–1585, https://doi.org/10.1016/j.ceramint.2011.01.023.
[53] C. Vitale-Brovarone, E. Vernè, M. Bosetti, P. Appendino, and M. Cannas, "Microstructural and in Vitro Characterization of SiO 2-Na 2 O-CaO-MgO Glass-Ceramic Bioactive Scaffolds for Bone Substitutes.".
[54] O. Lyckfeldt, J.M.F. Ferreira, Processing of porous ceramics by 'starch consolidation, J. Eur. Ceram. Soc. 18 (2) (1998) 131–140, https://doi.org/10.1016/S0955-2219(97)00101-5.
[55] A. Nommeots-Nomm, et al., Highly degradable porous melt-derived bioactive glass foam scaffolds for bone regeneration, Acta Biomater. 57 (2017) 449–461, https://doi.org/10.1016/j.actbio.2017.04.030.
[56] J.R. Jones, L.M. Ehrenfried, L.L. Hench, Optimising bioactive glass scaffolds for bone tissue engineering, Biomaterials 27 (7) (2006) 964–973, https://doi.org/10.1016/j.biomaterials.2005.07.017.
[57] G. Poologasundarampillai, P.D. Lee, C. Lam, A.-M. Kourkouta, J.R. Jones, Compressive strength of bioactive sol–gel glass foam scaffolds, Int. J. Appl. Glass Sci. 7 (2) (Jun. 2016) 229–237, https://doi.org/10.1111/ijag.12211.
[58] E. Boccardi, et al., Bioactivity and mechanical stability of 45S5 bioactive glass scaffolds based on natural marine sponges, Ann. Biomed. Eng. 44 (6) (Jun. 2016) 1881–1893, https://doi.org/10.1007/s10439-016-1595-5.
[59] Q.Z. Chen, I.D. Thompson, A.R. Boccaccini, 45S5 Bioglass®-derived glass–ceramic scaffolds for bone tissue engineering, Biomaterials 27 (11) (2006) 2414–2425, https://doi.org/10.1016/j.biomaterials.2005.11.025.
[60] Y.S. Park, et al., Feasibility of three-dimensional macroporous scaffold using calcium phosphate glass and polyurethane sponge, J. Mater. Sci. (Jul. 2006) 4357–4364, https://doi.org/10.1007/s10853-006-6261-0.
[61] F. Baino, C. Vitale-Brovarone, Mechanical properties and reliability of glass–ceramic foam scaffolds for bone repair, Mater. Lett. 118 (2014) 27–30, https://doi.org/10.1016/j.matlet.2013.12.037.
[62] Q. Fu, M.N. Rahaman, B. Sonny Bal, R.F. Brown, D.E. Day, Mechanical and in vitro performance of 13–93 bioactive glass scaffolds prepared by a polymer foam replication technique, Acta Biomater. 4 (6) (2008) 1854–1864, https://doi.org/10.1016/j.actbio.2008.04.019.
[63] X. Liu, N. Rahaman, Q. Fu, A. Tomsia, Porous and strong bioactive glass (13-93) scaffolds prepared by unidirectional freezing of camphene-based suspensions, Acta Biomater. 8 (Aug. 2011) 415–423, https://doi.org/10.1016/j.actbio.2011.07.034.
[64] V. Maquet, A.R. Boccaccini, L. Pravata, I. Notingher, R. Jérôme, Porous poly (α-hydroxyacid)/Bioglass® composite scaffolds for bone tissue engineering. I: preparation and in vitro characterisation, Biomaterials 25 (18) (2004) 4185–4194, https://doi.org/10.1016/j.biomaterials.2003.10.082.
[65] J.J. Blaker, V. Maquet, R. Jérôme, A.R. Boccaccini, S.N. Nazhat, Mechanical properties of highly porous PDLLA/Bioglass® composite foams as scaffolds for bone tissue engineering, Acta Biomater. 1 (6) (2005) 643–652, https://doi.org/10.1016/j.actbio.2005.07.003.
[66] K.K. Medicarbone, N. Doiphode, M.C. Leu, K.C.R. Kolan, N.D. Doiphode, Selective laser sintering and freeze extrusion fabrication of scaffolds for bone repair using 13-93 bioactive glass: a comparison [Online]. Available, https://www.researchgate.net/publication/266572710, 2010.
[67] F. Baino, et al., Digital light processing stereolithography of hydroxyapatite scaffolds with bone-like architecture, permeability, and mechanical properties, J. Am. Ceram. Soc. 105 (May 2021), https://doi.org/10.1111/jace.17843.
[68] F. Baino, J. Dias, M. Alidoost, M. Schwentenwein, E. Verné, Making foam-like bioactive glass scaffolds by vat photopolymerization, Open Ceramics 15 (2023) 100392, https://doi.org/10.1016/j.oceram.2023.100392.
[69] F. Baino, et al., Vat photopolymerization of ultra-porous bioactive glass foams, Open Ceramics 20 (2024) 100690, https://doi.org/10.1016/j.oceram.2024.100690.
[70] J. Barberi, et al., Robocasting of SiO_2-based bioactive glass scaffolds with porosity gradient for bone regeneration and potential load-bearing applications, Materials 12 (7) (2019), https://doi.org/10.3390/ma12172691.
[71] S. Eqtesadi, A. Motealleh, P. Miranda, A. Pajares, A. Lemos, J. Ferreira, Robocasting of 45S5 bioactive glass scaffolds for bone tissue engineering, J. Eur. Ceram. Soc. 34 (Jan. 2014) 107–118, https://doi.org/10.1016/j.jeurceramsoc.2013.08.003.
[72] X. Liu, M.N. Rahaman, G.E. Hilmas, B.S. Bal, Mechanical properties of bioactive glass (13-93) scaffolds fabricated by robotic deposition for structural bone repair, Acta Biomater. 9 (6) (2013) 7025–7034, https://doi.org/10.1016/j.actbio.2013.02.026.
[73] C. Wu, Y. Luo, G. Cuniberti, Y. Xiao, M. Gelinsky, Three-dimensional printing of hierarchical and tough mesoporous bioactive glass scaffolds with a controllable pore architecture, excellent mechanical strength and mineralization ability, Acta Biomater. 7 (6) (2011) 2644–2650, https://doi.org/10.1016/j.actbio.2011.03.009.
[74] P. Sepulveda, J.R. Jones, L.L. Hench, Bioactive sol-gel foams for tissue repair, J. Biomed. Mater. Res. 59 (2) (2002) 340–348, https://doi.org/10.1002/jbm.1250.
[75] J. Jones, L. Hench, Effect of surfactant concentration and composition on the structure and properties of sol-gel-derived bioactive glass foam scaffolds for tissue engineering, J. Mater. Sci. 38 (Sep. 2003) 3783–3790, https://doi.org/10.1023/A:1025988301542.
[76] E. Munch, M.E. Launey, D.H. Alsem, E. Saiz, A.P. Tomsia, R.O. Ritchie, Tough, bio-inspired hybrid materials, Science 322 (5907) (1979) 1516–1520, https://doi.org/10.1126/science.1164865. Dec. 2008.
[77] X. Liu, M.N. Rahaman, Q. Fu, Bone regeneration in strong porous bioactive glass (13-93) scaffolds with an oriented microstructure implanted in rat calvarial defects, Acta Biomater. 9 (1) (2013) 4889–4898, https://doi.org/10.1016/j.actbio.2012.08.029.
[78] E. Cunningham, et al., Comparative characterisation of 3-D hydroxyapatite scaffolds developed via replication of synthetic polymer foams and natural marine sponges, J. Tissue Sci. Eng. S1 (Jul. 2011) 1–9, https://doi.org/10.4172/2157-7552.S1-001.
[79] Q.Z. Chen, I.D. Thompson, A.R. Boccaccini, 45S5 Bioglass®-derived glass–ceramic scaffolds for bone tissue engineering, Biomaterials 27 (11) (Apr. 2006) 2414–2425, https://doi.org/10.1016/j.biomaterials.2005.11.025.
[80] E. Fiume, S. Ciavattini, E. Verné, F. Baino, Foam Replica Method in the Manufacturing of Bioactive Glass Scaffolds: Out-Of-Date Technology or Still Underexploited Potential? MDPI AG, 2021 https://doi.org/10.3390/ma14112795.
[81] K. Rezwan, Q.Z. Chen, J.J. Blaker, A.R. Boccaccini, Biodegradable and bioactive porous polymer/inorganic composite scaffolds for bone tissue engineering, Biomaterials 27 (18) (2006) 3413–3431, https://doi.org/10.1016/j.biomaterials.2006.01.039.
[82] R. Gmeiner, et al., Additive manufacturing of bioactive glasses and silicate bioceramics, J. Ceram. Sci. Technol. 6 (Jun. 2015) 75–86, https://doi.org/10.4416/JCST2015-00001.
[83] Z. Chen, et al., 3D printing of ceramics: a review, J. Eur. Ceram. Soc. 39 (4) (2019) 661–687, https://doi.org/10.1016/j.jeurceramsoc.2018.11.013.

[84] A. Kumar, K.C. Nune, R.D.K. Misra, Biological functionality of extracellular matrix-ornamented three-dimensional printed hydroxyapatite scaffolds, J. Biomed. Mater. Res. 104 (6) (Jun. 2016) 1343–1351, https://doi.org/10.1002/jbm.a.35664.
[85] S. Wu, X. Liu, K.W.K. Yeung, C. Liu, X. Yang, Biomimetic porous scaffolds for bone tissue engineering, Mater. Sci. Eng. R Rep. 80 (2014) 1–36, https://doi.org/10.1016/j.mser.2014.04.001.
[86] F. Baino, S. Caddeo, G. Novajra, C. Vitale-Brovarone, Using porous bioceramic scaffolds to model healthy and osteoporotic bone, J. Eur. Ceram. Soc. 36 (9) (Aug. 2016) 2175–2182, https://doi.org/10.1016/j.jeurceramsoc.2016.01.011.
[87] A. Kumar, S. Kargozar, F. Baino, S.S. Han, Additive manufacturing methods for producing hydroxyapatite and hydroxyapatite-based composite scaffolds: a review, Front Mater 6 (December) (2019) 1–20, https://doi.org/10.3389/fmats.2019.00313.
[88] R. Pugliese, S. Graziosi, Biomimetic scaffolds using triply periodic minimal surface-based porous structures for biomedical applications, SLAS Technol 28 (3) (Jun. 2023) 165–182, https://doi.org/10.1016/j.slast.2023.04.004.
[89] L.J. Gibson, M.F. Ashby, The mechanics of three-dimensional cellular materials, Proceedings of the Royal Society of London. A. Mathematical and Physical Sciences 382 (1782) (Jan. 1997) 43–59, https://doi.org/10.1098/rspa.1982.0088.
[90] S. Hollister, N. Kikuchi, A comparison of homogenization and standard mechanics analyses for periodic porous composites, Comput. Mech. 10 (Mar) (1992), https://doi.org/10.1007/BF00369853.
[91] E. Farina, et al., Micro computed tomography based finite element models for elastic and strength properties of 3D printed glass scaffolds, Acta Mech. Sin. 37 (Mar) (2021), https://doi.org/10.1007/s10409-021-01065-3.
[92] E. Cao, Z. Dong, X. Zhang, Z. Zhao, X. Zhao, H. Huang, Mechanical properties and failure analysis of 3D-printing micron-scale ceramic-based triply periodic minimal surface scaffolds under quasi-static-compression and low-speed impact loads, Compos. Sci. Technol. 243 (2023) 110248, https://doi.org/10.1016/j.compscitech.2023.110248.
[93] Z. Miri, et al., Review on the strategies to improve the mechanical strength of highly porous bone bioceramic scaffolds, J. Eur. Ceram. Soc. 44 (1) (2024) 23–42, https://doi.org/10.1016/j.jeurceramsoc.2023.09.003.
[94] E. Fiume, G. Serino, C. Bignardi, E. Verné, F. Baino, Sintering behavior of a six-oxide silicate bioactive glass for scaffold manufacturing, Appl. Sci. 10 (22) (Nov. 2020) 1–15, https://doi.org/10.3390/app10228279.
[95] L. D'Andrea, A. De Cet, D. Gastaldi, F. Baino, E. Verné, P. Vena, Estimation of elastic modulus, fracture toughness and strength of 47.5B-derived bioactive glass-ceramics for bone scaffold applications: a nanoindentation study, Mater. Lett. 335 (Mar) (2023), https://doi.org/10.1016/j.matlet.2022.133783.
[96] L. D'Andrea, et al., Mechanical characterization of miniaturized 3D-printed hydroxyapatite parts obtained through vat photopolymerization: an experimental study, J. Mech. Behav. Biomed. Mater. 141 (May 2023) 105760, https://doi.org/10.1016/j.jmbbm.2023.105760.
[97] O.A. Osuchukwu, et al., Weibull analysis of ceramics and related materials: a review, Heliyon 10 (12) (Jun. 2024) e32495, https://doi.org/10.1016/j.heliyon.2024.e32495.
[98] A. Entezari, S.I. Roohani-Esfahani, Z. Zhang, H. Zreiqat, C.R. Dunstan, Q. Li, Fracture behaviors of ceramic tissue scaffolds for load bearing applications, Sci. Rep. 6 (Jul) (2016), https://doi.org/10.1038/srep28816.
[99] C. Petit, et al., Fracture behavior of robocast HA/beta-TCP scaffolds studied by X-ray tomography and finite element modeling Fracture behavior of robocast HA/β-TCP scaffolds studied by X-ray tomography and finite element modeling, J. Eur. Ceram. Soc. 37 (4) (2017) 1735–1780, https://doi.org/10.1016/j.jeurceramsoc.2016.11.035ï.
[100] L. D'Andrea, et al., Computational models for the simulation of the elastic and fracture properties of highly porous 3D-printed hydroxyapatite scaffolds, Int J Numer Method Biomed Eng 40 (2) (Feb. 2024) e3795, https://doi.org/10.1002/cnm.3795.
[101] A. De Cet, et al., Micro-CT imaging and finite element models reveal how sintering temperature affects the microstructure and strength of bioactive glass-derived scaffolds, Sci. Rep. 14 (1) (2024) 969, https://doi.org/10.1038/s41598-023-50255-5.
[102] L. D'Andrea, et al., Mechanical properties of robocast glass scaffolds assessed through micro-CT-based finite element models, Materials 15 (18) (Sep. 2022), https://doi.org/10.3390/ma15186344.
[103] I. Touaiher, M. Saadaoui, P. Reynaud, H. Reveron, J. Chevalier, Mechanical properties of additive-manufactured hydroxyapatite porous scaffolds and follow-up of damage process under compression loading, Open Ceramics 16 (Dec. 2023), https://doi.org/10.1016/j.oceram.2023.100498.
[104] S. Ibrahimi, L. D'Andrea, D. Gastaldi, M. Rivolta, P. Vena, Machine Learning approaches for the design of biomechanically compatible bone tissue engineering scaffolds, Comput. Methods Appl. Mech. Eng. 423 (Apr. 2024) 116842, https://doi.org/10.1016/j.cma.2024.116842.
[105] A. Entezari, et al., Nondeterministic multiobjective optimization of 3D printed ceramic tissue scaffolds, J. Mech. Behav. Biomed. Mater. 138 (2023) 105580, https://doi.org/10.1016/j.jmbbm.2022.105580.
[106] W. Jia, G.Y. Lau, W. Huang, C. Zhang, A.P. Tomsia, Q. Fu, Bioactive glass for large bone repair, Adv. Healthcare Mater. 4 (18) (Dec. 2015) 2842–2848, https://doi.org/10.1002/adhm.201500447.
[107] V.I. dos Santos, J. Chevalier, M.C. Fredel, B. Henriques, L. Gremillard, Ceramics and ceramic composites for biomedical engineering applications via Direct Ink Writing: overall scenario, advances in the improvement of mechanical and biological properties and innovations, Mater. Sci. Eng. R Rep. 161 (Dec. 2024) 100841, https://doi.org/10.1016/j.mser.2024.100841.
[108] L. D'Andrea, T. Yang, M. Dao, P. Vena, Nature-inspired Orientation-dependent Toughening Mechanism for TPMS Ceramic Architectures, vol. 50, Apr. 2025, https://doi.org/10.1557/s43577-024-00831-5.
[109] Q. Fu, W. Jia, G.Y. Lau, A.P. Tomsia, Strength, toughness, and reliability of a porous glass/biopolymer composite scaffold, J. Biomed. Mater. Res. B Appl. Biomater. 106 (3) (Apr. 2018) 1209–1217, https://doi.org/10.1002/jbm.b.33924.
[110] F.J. O'Brien, B.A. Harley, M.A. Waller, I. V Yannas, L.J. Gibson, P.J. Prendergast, The effect of pore size on permeability and cell attachment in collagen scaffolds for tissue engineering, Technol. Health Care 15 (2007) 3–17, https://doi.org/10.3233/THC-2007-15102.
[111] S. Gómez, M.D. Vlad, J. López, E. Fernández, Design and properties of 3D scaffolds for bone tissue engineering, Acta Biomater. 42 (2016) 341–350, https://doi.org/10.1016/j.actbio.2016.06.032.
[112] R. Asbai-Ghoudan, S. Ruiz de Galarreta, N. Rodriguez-Florez, Analytical model for the prediction of permeability of triply periodic minimal surfaces, J. Mech. Behav. Biomed. Mater. 124 (Dec) (2021), https://doi.org/10.1016/j.jmbbm.2021.104804.
[113] A.H. Foroughi, M.J. Razavi, Multi-objective shape optimization of bone scaffolds: enhancement of mechanical properties and permeability, Acta Biomater. 146 (Jul. 2022) 317–340, https://doi.org/10.1016/j.actbio.2022.04.051.
[114] R. Huiskes, W.D. Van Driel, P.J. Prendergast, K. Søballe, A biomechanical regulatory model for periprosthetic fibrous-tissue differentiation, in: Journal of Materials Science: Materials in Medicine, Chapman & Hall Ltd, Dec. 1997, pp. 785–788, https://doi.org/10.1023/A:1018520914512.
[115] O. Faweya, P.S. Desai, C.F. Higgs, Towards an agent-based model to simulate osseointegration in powder-bed 3D printed implant-like structures, J. Mech. Behav. Biomed. Mater. 126 (Feb) (2022), https://doi.org/10.1016/j.jmbbm.2021.104915.
[116] P.F. Egan, K.A. Shea, S.J. Ferguson, Simulated tissue growth for 3D printed scaffolds, Biomech. Model. Mechanobiol. 17 (5) (Oct. 2018) 1481–1495, https://doi.org/10.1007/s10237-018-1040-9.
[117] S.J.P. Callens, et al., Emergent collective organization of bone cells in complex curvature fields, Nat. Commun. 14 (1) (Dec. 2023), https://doi.org/10.1038/s41467-023-36436-w.
[118] Y. Zhang, et al., In silico and in vivo studies of the effect of surface curvature on the osteoconduction of porous scaffolds, Biotechnol. Bioeng. 119 (2) (Feb. 2022) 591–604, https://doi.org/10.1002/bit.27976.
[119] M. Mirkhalaf, Y. Men, R. Wang, Y. No, H. Zreiqat, Personalized 3D printed bone scaffolds: a review, Acta Biomater. 156 (2023) 110–124, https://doi.org/10.1016/j.actbio.2022.04.014.
[120] J.A. Sanz-Herrera, A.R. Boccaccini, Modelling bioactivity and degradation of bioactive glass based tissue engineering scaffolds, Int. J. Solid Struct. 48 (2) (Jan. 2011) 257–268, https://doi.org/10.1016/j.ijsolstr.2010.09.025.
[121] M. Bahraminasab, Challenges on optimization of 3D-printed bone scaffolds, Biomed. Eng. Online 19 (1) (2020) 1–33, https://doi.org/10.1186/s12938-020-00810-2.
[122] J. Kim, J.A. McKee, J.J. Fontenot, J.P. Jung, Engineering tissue fabrication with machine intelligence: generating a blueprint for regeneration, Front. Bioeng. Biotechnol. 7 (January) (2020) 1–9, https://doi.org/10.3389/fbioe.2019.00443.
[123] J. Wu, Y. Zhang, Y. Lyu, L. Cheng, On the Various Numerical Techniques for the Optimization of Bone Scaffold, MDPI, Feb. 01, 2023, https://doi.org/10.3390/ma16030974.
[124] O. Ronneberger, P. Fischer, T. Brox, U-net: Convolutional Networks for Biomedical Image Segmentation, vol. 9351, 2015, https://doi.org/10.1007/978-3-319-24574-4_28.
[125] A. de M.B. Junior, A. D. Dó Neto, J.D. de Melo, L.M.G. Goncalves, An adaptive learning approach for 3-D surface reconstruction from point clouds, IEEE Trans. Neural Network. 19 (6) (2008) 1130–1140, https://doi.org/10.1109/TNN.2008.2000390.
[126] H. Sun, H. Al-Marzouqi, S. Vega, EPCI: a new tool for predicting absolute permeability from computed tomography images, Geophysics 84 (3) (Feb. 2019) F97–F102, https://doi.org/10.1190/geo2018-0653.1.
[127] M. Genet, M. Houmard, S. Eslava, E. Saiz, A.P. Tomsia, A two-scale Weibull approach to the failure of porous ceramic structures made by robocasting: possibilities and limits, J. Eur. Ceram. Soc. 33 (4) (2013) 679–688, https://doi.org/10.1016/j.jeurceramsoc.2012.11.001.
[128] G. Drakoulas, T. Gortsas, E. Polyzos, S. Tsinopoulos, L. Pyl, D. Polyzos, An explainable machine learning-based probabilistic framework for the design of scaffolds in bone tissue engineering, Biomech. Model. Mechanobiol. 23 (3) (Jun. 2024) 987–1012, https://doi.org/10.1007/s10237-024-01817-7.
[129] C. Wu, B. Wan, A. Entezari, J. Fang, Y. Xu, Q. Li, Machine learning-based design for additive manufacturing in biomedical engineering, Int. J. Mech. Sci. 266 (2024) 108828, https://doi.org/10.1016/j.ijmecsci.2023.108828.
[130] T. Smit, N. Aage, D. Haschtmann, S.J. Ferguson, B. Helgason, Anatomically and mechanically conforming patient-specific spinal fusion cages designed by full-scale topology optimization, J. Mech. Behav. Biomed. Mater. 159 (Nov. 2024) 106695, https://doi.org/10.1016/j.jmbbm.2024.106695.
[131] G. Kaur, et al., Mechanical properties of bioactive glasses, ceramics, glass-ceramics and composites: state-of-the-art review and future challenges, Mater. Sci. Eng. C 104 (2019) 109895, https://doi.org/10.1016/j.msec.2019.109895.
[132] T. Hildebrand, A. Laib, R. Müller, J. Dequeker, P. Rüegsegger, Direct three-dimensional morphometric analysis of human cancellous bone: microstructural

data from spine, femur, iliac crest, and calcaneus, J. Bone Miner. Res. 14 (7) (Jul. 1999) 1167–1174, https://doi.org/10.1359/jbmr.1999.14.7.1167.
[133] T.M. Link, et al., Structure analysis of high resolution magnetic resonance imaging of the proximal femur: in vitro correlation with biomechanical strength and BMD, Calcif. Tissue Int. 72 (2) (Feb. 2003) 156–165, https://doi.org/10.1007/s00223-001-2132-5.
[134] J.R. Jones, R.C. Atwood, G. Poologasundarampillai, S. Yue, P.D. Lee, Quantifying the 3D macrostructure of tissue scaffolds, J. Mater. Sci. Mater. Med. (Feb. 2009) 463–471, https://doi.org/10.1007/s10856-008-3597-9.
[135] S. J. Hollister, E. E. Liao, E. N. Moffitt, C. G. Jeong, and J. M. Kemppainen, "Defining Design Targets for Tissue Engineering Scaffolds.".
[136] S.M.M. Roosa, J.M. Kemppainen, E.N. Moffitt, P.H. Krebsbach, S.J. Hollister, The pore size of polycaprolactone scaffolds has limited influence on bone regeneration in an in vivo model, J. Biomed. Mater. Res. 92A (1) (Jan. 2010) 359–368, https://doi.org/10.1002/jbm.a.32381.
[137] M. Bohner, Y. Loosli, G. Baroud, D. Lacroix, Commentary: deciphering the link between architecture and biological response of a bone graft substitute, Acta Biomater. 7 (2) (2011) 478–484, https://doi.org/10.1016/j.actbio.2010.08.008.
[138] J. Li, et al., Bone induction by surface-double-modified true bone ceramics in vitro and in vivo, Biomed. Mater. 8 (3) (2013) 035005, https://doi.org/10.1088/1748-6041/8/3/035005.
[139] Y. Jiang, et al., True-bone-ceramics/type I collagen scaffolds for repairing osteochondral defect, J. Mater. Sci. Mater. Med. 36 (1) (2024) 1, https://doi.org/10.1007/s10856-024-06852-5.
[140] G. Falvo D'Urso Labate, G. Catapano, C. Vitale-Brovarone, F. Baino, Quantifying the micro-architectural similarity of bioceramic scaffolds to bone, Ceram. Int. 43 (Apr. 2017) 9443–9450, https://doi.org/10.1016/j.ceramint.2017.04.121.
[141] G. Falvo D'Urso Labate, et al., Bone structural similarity score: a multiparametric tool to match properties of biomimetic bone substitutes with their target tissues, Journal of Applied Biomaterials and Fundamental Materials 14 (Jul. 2016) e277–e289, https://doi.org/10.5301/jabfm.5000283.
[142] M.J. White, Segregation and diversity measures in population distribution, Popul. Index 52 (2) (1986) 198–221, https://doi.org/10.2307/3644339.
[143] T. Van Cleynenbreugel, J. Schrooten, H. Van Oosterwyck, J. Vander Sloten, Micro-CT-based screening of biomechanical and structural properties of bone tissue engineering scaffolds, Med. Biol. Eng. Comput. 44 (7) (Jul. 2006) 517–525, https://doi.org/10.1007/s11517-006-0071-z.
[144] F. Baino, G. Falvo D'Urso Labate, G.G. di Confiengo, M.G. Faga, C. Vitale-Brovarone, G. Catapano, Microstructural characterization and robust comparison of ceramic porous orbital implants, J. Eur. Ceram. Soc. 38 (8) (Jul. 2018) 2988–2993, https://doi.org/10.1016/j.jeurceramsoc.2017.12.047.
[145] F. Pennella, et al., A survey of methods for the evaluation of tissue engineering scaffold permeability, Ann. Biomed. Eng. 41 (10) (Oct. 2013) 2027–2041, https://doi.org/10.1007/s10439-013-0815-5.
[146] R. Gabrieli, A. Schiavi, F. Baino, Determining the Permeability of Porous Bioceramic Scaffolds: Significance, Overview of Current Methods and Challenges Ahead, Multidisciplinary Digital Publishing Institute (MDPI), Nov. 01, 2024, https://doi.org/10.3390/ma17225522.
[147] J.R. Jones, G. Poologasundarampillai, R.C. Atwood, D. Bernard, P.D. Lee, Non-destructive quantitative 3D analysis for the optimisation of tissue scaffolds, Biomaterials 28 (7) (2007) 1404–1413, https://doi.org/10.1016/j.biomaterials.2006.11.014.
[148] I. Ochoa, J.A. Sanz-Herrera, J.M. García-Aznar, M. Doblaré, D.M. Yunos, A. R. Boccaccini, Permeability evaluation of 45S5 Bioglass®-based scaffolds for bone tissue engineering, J. Biomech. 42 (3) (2009) 257–260, https://doi.org/10.1016/j.jbiomech.2008.10.030.
[149] Standard Guide for Determining the Mean Darcy Permeability Coefficient for a Porous Tissue Scaffold 1", doi: 10.1520/F2952-14.
[150] A. Schiavi, E. Fiume, G. Orlygsson, M. Schwentenwein, E. Verné, F. Baino, High-reliability data processing and calculation of microstructural parameters in hydroxyapatite scaffolds produced by vat photopolymerization, J. Eur. Ceram. Soc. 42 (13) (Oct. 2022) 6206–6212, https://doi.org/10.1016/j.jeurceramsoc.2022.06.022.
[151] A. Schiavi, R. Gabrieli, G. Orlygsson, M. Schwentenwein, E. Verné, F. Baino, Assessment of permeability and microstructural parameters via fractal modelling in bioactive glass-derived scaffolds produced by vat photopolymerization, J. Eur. Ceram. Soc. 44 (7) (2024) 4689–4698, https://doi.org/10.1016/j.jeurceramsoc.2024.01.095.
[152] J. Wu, B. Yu, M. Yun, A resistance model for flow through porous media, Transport Porous Media 71 (Feb. 2008) 331–343, https://doi.org/10.1007/s11242-007-9129-0.
[153] W. Guo, B. Li, P. Li, L. Zhao, H. You, Y. Long, Review on vat photopolymerization additive manufacturing of bioactive ceramic bone scaffolds, J. Mater. Chem. B 11 (40) (2023) 9572–9596, https://doi.org/10.1039/D3TB01236K.
[154] A. Gupta, S. Babu L, Triply periodic minimal surfaces: an overview of their features, failure mechanisms, and applications, J. Mine Met. Fuel (Mar. 2023) 211–221, https://doi.org/10.18311/jmmf/2022/31230.
[155] H. Jinnai, H. Watashiba, T. Kajihara, Y. Nishikawa, M. Takahashi, M. Ito, Surface curvatures of trabecular bone microarchitecture, Bone 30 (1) (2002) 191–194, https://doi.org/10.1016/S8756-3282(01)00672-X.
[156] C. Schmidleithner, S. Malferrari, R. Palgrave, D. Bomze, M. Schwentenwein, D. M. Kalaskar, Application of high resolution DLP stereolithography for fabrication of tricalcium phosphate scaffolds for bone regeneration, Biomed. Mater. 14 (4) (Jun. 2019), https://doi.org/10.1088/1748-605X/ab279d.
[157] M. Paris, et al., Scaffold curvature-mediated novel biomineralization process originates a continuous soft tissue-to-bone interface, Acta Biomater. 60 (2017) 64–80, https://doi.org/10.1016/j.actbio.2017.07.029.
[158] M.A. Alias, P.R. Buenzli, Modeling the effect of curvature on the collective behavior of cells growing new tissue, Biophys. J. 112 (1) (2017) 193–204, https://doi.org/10.1016/j.bpj.2016.11.3203.
[159] W. Roque, K. Arcaro, A. Alberich-Bayarri, Mechanical competence of bone: a new parameter to grade trabecular bone fragility from tortuosity and elasticity, IEEE Trans. Biomed. Eng. 60 (Dec) (2012), https://doi.org/10.1109/TBME.2012.2234457.